Functional Characterization of the Helicase Domain of Active DNA-Dependent ATPase A

Dissertation Submitted to
Jawaharlal Nehru University
For the Award of the Degree of

MASTER OF PHILOSOPHY

Macmillan Nongkhlaw

School of Life Sciences
Jawaharlal Nehru University
New Delhi 110067
INDIA

2006

Contents

School Of Life Sciences
Jawaharlal Nehru University
New Delhi 110 067 India

Certificate

The dissertation work embodied in this thesis entitled ***"Functional Characterization of the Helicase Domain of Active DNA-Dependent ATPase A"*** *has been carried out at the School of Life Sciences, Jawaharlal Nehru University, New Delhi, India. This work is original and has not been submitted so far, in part or in full for the award of any other degree or diploma in any other university.*

Supervisor

(Dr. Rohini Mathuswami)

Candidate

(Macmillan Nongkhlaw)

Dean

(Prof. R. N.K. Bamezai)

ACKNOWLEDGEMENT

At the very outset, I sincerely acknowledge with deep faith the omnipotent help of God the Almighty without whose grace and blessings all my endeavors would have borne no fruit.

My utmost sense of gratitude goes to my supervisor, Dr. Rohini Muthuswami, who has always been a source of encouragement and support. I am especially indebted to her for her patience and guidance through out the course of my project. Working under her has been a great and joyful experience in many ways.

My special thanks goes to Dr. Sneha Sudha Komath for her help and suggestions in my experiments.

I owe my most sincere gratitude to my Parents, my brothers and sisters for all their love and concern. Their support shall forever remain an immeasurable source of strength for me

I thank Prof. R. N. K. Bamezai, Dean, SLS for providing with necessary facility to carry out this investigation.

The staff of Central instruments facility (CIF), Central computer instruments facility (CCIF) and the administrative staff of School of Life Sciences have a share in the success of this endeavor. Special thanks are due to Mrs. Meenu Madam whose loving disposition endears her to all who know her.

I am grateful to all my lab mates; Pravin, Soraya, Popy, Reshma Hemant, Ramesh, Ashraf, for their consistent help, suggestions and enlightened friendly company.

I express my thanks to Bishenji, and Ashu for their ever-ready and helpful presence.

My thanks also goes to the DBT for providing me with financial assistance.

Last but not the least, I salute all my friends around: Badap, Ferdinand, Pynskhem, Pyniar, Teibor, Moses, Chanchal and others for all the exciting moments and experiences, making my stay in JNU a very joyful one.

MAY GOD BLESS YOU ALL !

List of Figures

List of Tables

Abbreviations

ADAAD	Active DNA-Dependent ATPase A
ATP	Adenosine triphosphate
dNTP	deoxy-Nucleotide triphosphate
bp	Base pair
CSB	Cockayne Syndrome B
CHD	Chromodomain
DNA	Deoxyribonucleic acid
DTT	Dithiothreitol
EDTA	Ethylene diamine tetraacetate
FLADAAD	Full length ADAAD
GST	Glutathione-S-transferase
IPTG	Isopropyl-β-D-thiogalactopyranoside
ISWI	Imitation SWI
kb	Kilobase
kDa	Kilo Dalton
L	Litre
LB	Luria Broth
ml	milliliter
MAD	mutant ADAAD
mM	millimolar
nM	nanomolar
OD	Optical Density
PAGE	Polyacrylamide gel electrophoresis
PBS	Phosphate buffer saline
PCR	Polymerase Chain Reaction
PEP	Phosphoenol pyruvate
PMSF	Phenylmethylsulfonyl fluoride
rpm	revolutions per minute
SDS	Sodium dodecyl sulphate
SF	Superfamily
SMARCAL1	SWI/SNF-related matrix associated actin dependent regulator of chromatin subfamily a-like 1
SNF	Sucrose non-fermenting
SWI	mating type switching
µl	microliter
µg	microgram

INTRODUCTION

Eukaryotic DNA is wrapped around a condensed nucleoprotein complex which is called the chromatin. The chromatin structure is based on a repeating unit of eight histone molecules and about 200 DNA base pairs. This structure restricts the interaction of DNA with most nuclear factors. Important nuclear processes like transcription, replication, recombination and repair need accessibility to the DNA molecule. During these processes, chromatin structure is assembled and disassembled by different enzymes.

In an actively dividing eukaryotic cell chromatin disruption occurs during DNA replication DNA repair recombination (14) and transcription (30, 59, 65) which has wider implications throughout the life of the cell. The various enzymes found involved in the assembly and disassembly of the chromatin can be classified into two groups. These two groups of enzymes are: i) Histone modifying enzymes including histone acetyltransferase (HAT) and histone deacetylase (HDAC) complexes, which regulate the transcriptional activity of genes by determining the level of acetylation of the amino terminal domains of nucleosomal histones associated with them. ii) ATP-dependent complexes, which use the energy of ATP hydrolysis to locally disrupt or alter the association of histones with DNA(5, 60).

We will, in this chapter, understand the organization of the chromatin and the importance of remodeling systems for DNA metabolic processes.

Chromatin organization

The basic unit of the nucleosome is the four histone proteins H2A, H2B, H3 and H4 which form an octamer amongst themselves. The histones molecules carry a net positive charge which helps in packaging of negatively charged DNA.

Crystal structure of the histone octamer has shown that it possesses a tripartite organization i.e. a centrally located (H3-H4)2 is flanked by two H2A-H2B dimers(2). The three subunits are assembled in the form of a left-handed protein superhelix with an apparent pitch of 28Å and form a solid object with a small central cavity(2, 3). These studies further revealed that 146 base pair of the DNA was wrapped around the octamer with a 1.65 superhelical turn (40). This arrangement leads to about 6-fold packing of the DNA in the cell(33, 51). This repeating unit of chromatin is successively packaged into higher order structures achieving additional levels of compaction(51). This compaction involves the action of histone H1, which binds to DNA on the outside of nucleosomes (at a ratio of one H1 molecule per nucleosome), thus connecting nucleosomes. The linker DNA wrapped up by H1 could vary in length between 20-60 base pairs. Higher order compaction is achieved when H1 molecules interact with each other, causing the chromatin to form a spiral, with 6 to 8 nucleosomes per turn of the spiral. This structure is known as a solenoid or a 30 nm chromatin fiber(51). Even higher order compaction is achieved by chromatin looping as envisaged by electron micrograph of metaphase chromatin.

Packaging of DNA into these higher order structures renders it inaccessible to transcription and other nuclear processes.

Chromatin Remodeling

The inaccessible DNA is made accessible through the process of chromatin remodeling. Two major classes of chromatin remodeling complexes- histone-modifying enzymes and ATP-dependent chromatin remodeling proteins- regulate accessibility of the template to DNA binding factors. Histone-modifying enzymes are involved in covalent

modification of nucleosomes by adding or removing many chemical moieties by acetylation, phosphorylation, and methylation of histone N-termini(1). ATP-dependent chromatin remodeling proteins can move nucleosomes, thereby exposing or occluding DNA sequences, and creating conformations where DNA is accessible on the surface of the histone octamer(41). In this chapter we will be focusing on the ATP-dependent chromatin remodeling process.

ATP-dependent Chromatin Remodeling

ATP-dependent chromatin remodeling is one of the commonly used mechanisms to remodel chromatin. In this method energy released from ATP hydrolysis is utilized to mobilize and reposition nucleosomes, thereby exposing the DNA to various transcription factors and other DNA binding proteins (5, 60).

The SWI/SNF family of chromatin remodelers was first discovered in yeast through genetic screens that led to the identification of the so-called swi (*swi*tch) or snf (*s*ucrose *n*on*f*ermenting) mutations (54). The similarity of phenotypes conferred by mutations in different components of the complex suggested that many of the proteins encoded by these genes function in a coordinated manner. Homology searches with the sequence of the yeast Snf2p ATPase and biochemical scrutiny led to the identification of several SWI/SNF-related nucleosome remodeling machines in higher eukaryotes.

Chromatin-remodeling complexes are compositionally and functionally diverse, yet they share the presence of a motor domain that belongs to the Snf2-like family of ATPases. The motor domain is responsible for hydrolysis of ATP in the presence of DNA. The ATPase motor domains of the SWI/SNF proteins belong to the DEAD/H superfamily of nucleic acid stimulated ATPase, a large protein superfamily that includes

helicases. This protein superfamily is further classified into superfamily 1, 2, 3, and 4. Super family 2 (SF2) comprises of those proteins which possess the seven helicase motifs. It is the largest of the four superfamilies of helicases and includes a variety of DNA helicases and several families of RNA helicases and DNA-stimulated ATPase (25). The SWI/SNF proteins possess the ATPase motor domain that carries the entire seven helicase motifs. These proteins show DNA-stimulated ATP hydrolysis activity which is similar to helicase. However, unlike helicase they do not have helicase activity(37).

Recently, crystal structures of some SWI/SNF motor domain have been determined. These crystal structure studies show that motor domain possess a bi-lobed structure separated by a deep cleft. Comparative studies with some of the already crytallised helicases have revealed the structural and functional difference between the ATPase domain of SWI/SNF and that of helicases (18, 56).

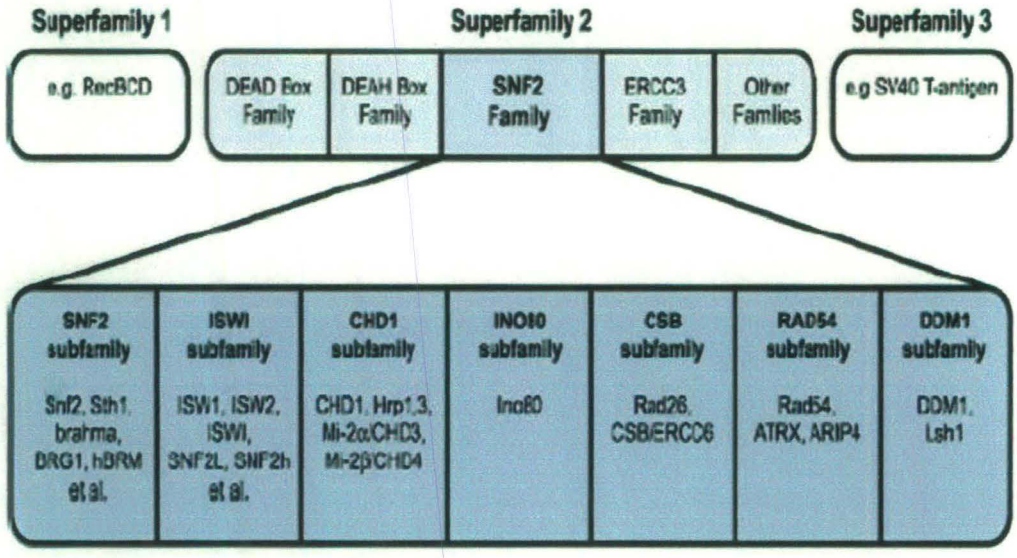

Figure 1: The SNF2-like family of ATPases includes many proteins that are involved in chromatin remodeling(41).

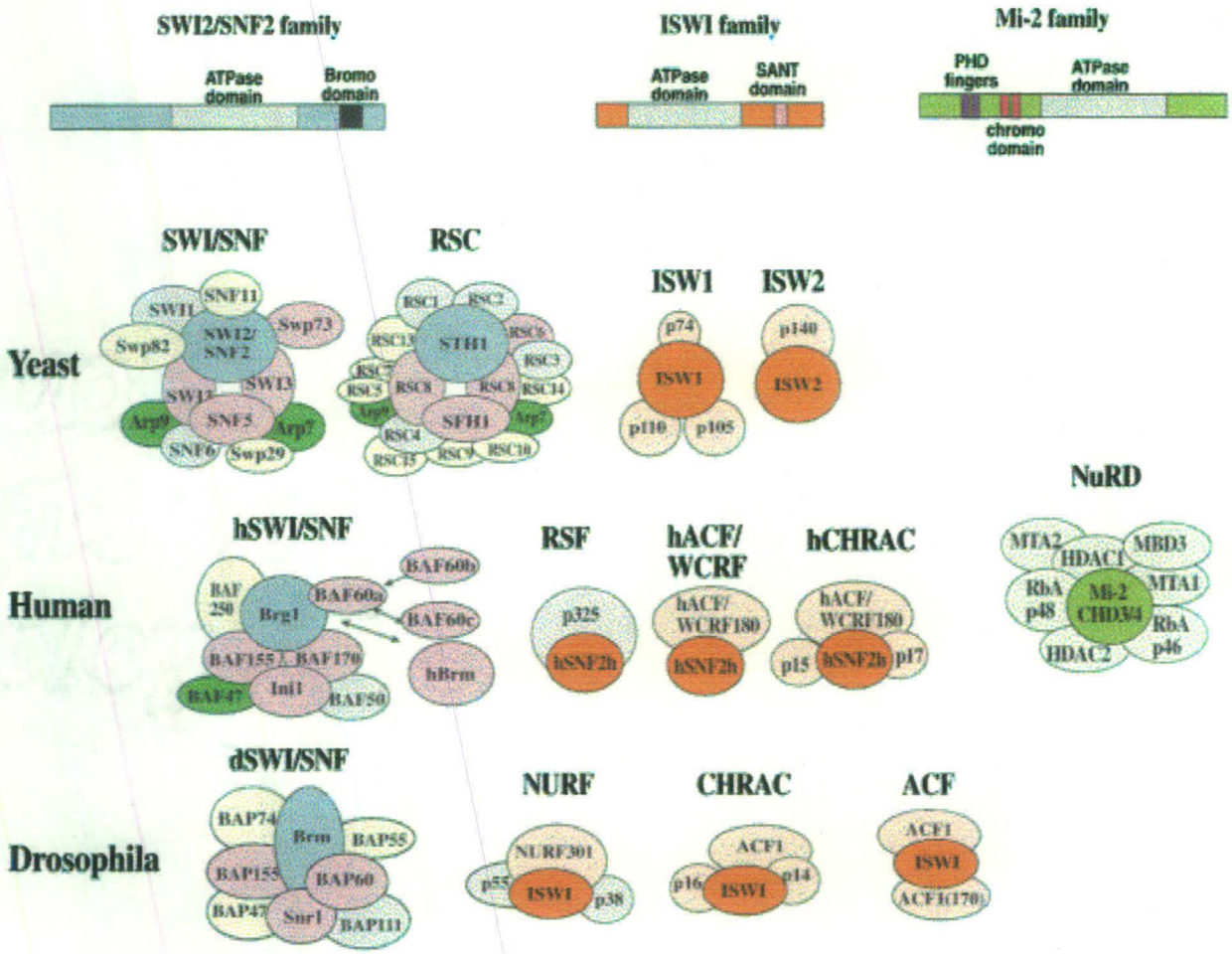

Figure 2: ATP-Dependent Remodeling Complexes(45)

SWI/SNF Complex

The SWI/SNF complex was first discovered in *Saccharomyces cerevisiae*, beginning with two genetic screens for altered gene expression, which led to the isolation of mutants with various phenotypes(12, 54). Genetic analysis and sequence identity led to the recognition that SNF2 (SWI2), SNF5, SNF6, SWI1, and SWI3 constitute a group of functionally related proteins. These genes are non-essential for viability, but mutations

affect transcription of a broad range of differently regulated genes, implying a global role in transcription control(11).

Mutations in *SNF* genes were identified as causing defects in expression of the *SUC2* gene, which is required for growth on sucrose and raffinose as carbon sources (the name Snf is derived from sucrose non fermenter)(12). Similarly, mutations in *SWI* genes were identified as defective for expression of the *HO* gene, which is required for mating type switching (the name Swi is derived from switching defective)(54). Mutations in both *SNF* and *SWI* genes cause pleiotropic phenotypes, suggesting a global role for SWI/SNF in gene expression (11).

SWI/SNF was initially linked to chromatin structure by the isolation of suppressors of *swi/snf* mutations in genes encoding histones and other putative chromatin components. The connection was strengthened by the finding that SWI/SNF is required *in vivo* for obtaining a transcriptionally active chromatin structure, as judged by increased nuclease sensitivity at the *SUC2* promoter(65). *In vitro* studies demonstrated that SWI/SNF complexes could cause ATP-dependent disruption of nucleosome structure leading to increase binding of transcription factors to their sites on nucleosomal templates, and thereby providing biochemical evidence for a role for SWI/SNF in nucleosome remodeling. These genetic and biochemical analyses led to the model that SWI/SNF controls transcription *in vivo* by disrupting nucleosome structure at the promoter and by facilitating the binding of transcription factors to their respective sites(34). SWI/SNF function is conserved in eukaryotes, as related complexes have been discovered in *S. cerevisiae*, *Drosophila melanogaster* and humans (Table1).

Table 1. Known subunits of the SWI2/SNF2 group of ATP-dependent chromatin-remodeling complexes(60).

Yeast SWI/SNF	Yeast RSC	*Drosphila* Brahma	Human SWI/SNF
Swi2/Snf2	Sth1/Nsp1	Brm	hBRG1 or hBRM
Swi1			p270(?)/BAF250
Snf5	Sfh1	Snr1	hSNF5/INI1/BAF47
Swi3	Rsc8/Swh3	Bap155/Moira	BAF170, BAF155
Swp82			
Swp73/Snf12	Rsc6	Bap60	BAF60 (a,b,c)
Swp61/Arp7	Rsc11/Arp7	Bap55 (?)	BAF53 (?)
Swp59/Arp9	Rsc12/Arp9	Bap55 (?)	BAF53 (?)
Snf6			
Swp29/$Taf_{II}30$			
Snf11			
	Rsc1 or -2		
	Rsc3-5,-7,-9,-10		
	Rsc13-15		
		Bap111	BAF57
		β-Actin/Bap47 (*)	β-Actin (*)
		Bap74	

The SWI/SNF complex in *S. cerevisiae* is a large multi-subunit complex comprising of 11 subunits. Five units have been identified genetically SWI3/SNF2, SWI1, SWI3, SNF5 and SNF7(10). The remaining six subunits were found in a biochemically isolated complex: SWP82, SWP73, SWP 61, SWP59, TAFII30 and SNF1 (ref?). The motor of this complex is the nucleosome remodeling ATPase -Snf2p-which is a 200-kDa protein(37, 63). The function of many of the other subunits is less well understood. Swi1 contains an AT-rich interaction domain (ARID) that allows nonspecific DNA binding (64). Targeted mutations in SNF5, one of the core subunits also conserved in higher eukaryotes, showed that it is involved in both assembly and catalytic functions of the complex(24). Interestingly, SWI/SNF complexes in yeast and

higher eukaryotes contain the actin-related proteins Arp7 and Arp9. It has been suggested that they might actually provide a link to nuclear structures, such as the nuclear matrix.(5).

Homology searches with the sequence of the yeast Snf2p ATPase and biochemical scrutiny led to the identification of several SWI/SNF-related nucleosome remodeling machines in higher eukaryotes(46). The *D. melanogaster* and mammalian complexes all contain subunits that are homologous to the yeast SWI2/SNF2, SWI3, SNF5, and SWP73 subunits as well as the above-mentioned actin-related proteins (5, 46). The homology of these proteins extends beyond the ATPase domain, as they all contain a bromodomain in the C-terminal region and two other conserved regions of unknown function called domains 1 and 2. Also all these proteins were found to contain the helicase motifs found in DNA and RNA helicase, but these proteins lack detectable DNA helicase and DNA tracking activities(10, 37).

Like yeast, human cells have at least two SWI/SNF-related complexes, referred to as BAF (hSwi/Snf-A or BRG1 complex) and PBAF (hSwi/Snf-B or hBRM complex). The corresponding ATPase subunits of these complexes, BRG1 and hBRM, are highly homologous to each other and to yeast Snf2. The other proteins in these complexes have been termed hBRM- and BRG1-associated factors (BAFs) and are again quite similar to each other(62). BRG1 and hBRM alone are able to carry out various nucleosome remodeling reactions, but the efficiency of remodeling is increased in the presence of other subunits.

Proteins of the SNF2 Family

Proteins belonging to the SWI/SNF family are subdivided into several sub families on the basis of similarity in conserved structural motifs(19, 25). Three main groups have been identified: the SWI/SNF group, the imitation SWI/SNF (ISWI) group and the Mi-2 group(57, 58). ATPases motor domain of the SWI2 group contains a bromodomain, whereas ISWI-like ATPases feature a SANT domain. CHD-type enzymes, such as Mi-2, contain chromodomains and PHD fingers(17, 58). These three groups can also be distinguished by their biochemical properties and mechanisms of nucleosome remodeling. In addition there are sub-families like INO80, Rad-54, and SMARCAL1(21).

Proteins with helicase like region of similar primary sequence to *S. cerevisiae* Snf2p comprise the Snf2 sub-family. In addition to homology within the helicase domains, these proteins also contain the bromodomain, which can interact with acetylated histones(27). Furthermore, these proteins can bind to both naked DNA and nucleosomal DNA(16, 44).

ISWI (imitation SWI) contains, in addition to the motor domain, a SANT domain. ATPase activity in these complexes is stimulated by the nucleosome and not by naked DNA. It is hypothesized that these proteins may also bind DNA through the SANT domain. SANT (Swi3, Ada2, N-CoR and TFIIIB) is a domain that is found in many transcription activators and corepressors. The ISWI complex is essential for viability of Drosophila. NURF (nucleosome remodeling factor), CHRAC (chromatin assembly complex), and ACF (ATP-utilizing chromatin assembly and remodeling factor) are some of the members of the ISWI subfamily that have been isolated from Drosophila.

NURF can cause the movement of nucleosome along the DNA; CHRAC in addition to NURF activity can generate equally spaced nucleosomes (36). Yeast and human homologue of the ISWI have also been isolated recently(55, 58).

The CHD subfamily comprises of those protein that contain the chromodomain (chromatin organization modifier) and a DNA binding domain(17). Protein complexes that contain the chromodomain show both ATP-dependent nucleosome rearrangement and histones deacetylase activity. The chromodomain has been shown to bind to the chromatin possibly through methylated histones(57). Some complexes have additional activities including Me-CpG DNA binding activity(35).

The Ino subfamily was identified by the isolation of a novel complex from yeast that shares homology in its central domain with the Drosophila ISWI and yeast Snf2p(53). Ino80 has both Drosophila (dINO80) and human (hINO80) homologs and sequence alignments reveal that these proteins contain two conserved regions beyond the motor domain, a TELY motif at the amino terminus and a GTIE motif at the carboxy terminus. Ino80 does not contain a SANT domain or a bromodomain, which are motifs found in Snf2 and ISWI subfamilies. Ino80 was purified as a complex (named Ino80.com) with approximately 12 associated proteins. Notable subunits of Ino80.com include Rvb1 and Rvb2, which share homology to the bacterial RuvB helicase, andAct1/actin, Arp4, Arp5, and Arp8. Ino80.com was found to have a 3' to 5' DNA helicase activity using strand displacement assays, and Ino80 null mutants exhibited sensitivity to hydroxyurea, methyl methanesulfonate (MMS), ultraviolet light, and ionizing radiation, indicating roles for this complex in replication and/or the processing of DNA damage(53).

The CSB/ERCC sub-family comprises of those proteins which are involved in transcription-coupled repair(52). This family consists of the CSB protein and the *S. cerevisiae* homologue Rad26p. These proteins were found to be involved in helping RNA polymerase to pass or dissociate from blocking DNA lesions. The mechanism by which CSB remodels nucleosome is unknown, but by changing DNA conformation, CSB may disrupt the histone–DNA interaction, as well as the interaction of the stalled DNA polymerase with damage DNA (42). In *in vitro* assays purified ERCC6 can alter nuclease sensitivity and spacing of nucleosome in ATP-dependent manner(52).

Rad 54 was initially identified as a member of the Rad51 epistasis group in *S. cerevisiae*(56). Like other SWI/SNF proteins, Rad54 can translocate on DNA, generate superhelical torsion and enhance accessibility to nucleosomal DNA. Rad54 may be involved in the repair of double strand break through Rad52 mediated homologous recombination. The crystal structure of Rad54 helicase like protein from zebra fish has been determined recently(56)

The DDM1 sub family comprises of the widely-expressed Lsh (lymphoid specific helicase) protein, which is localized to heterochromatin regions of the chromosome. Lsh and its human homologue are alternatively known as PASG, SMARCA6 or by the official gene name HELLS (Helicase Lymphoid Specific). Mutations in this protein lead to premature aging with cells exhibiting replicative senescence. DDM1 is Arabidopsis thaliana homologue of Lsh. Evidence has been presented that *A. thaliana* DDM1 can slide nucleosomes *in vitro*(9).

Mechanism of action of the SWI/SNF complex

The mechanisms by which SWI/SNF complex alter chromosome and chromatin structure are not yet clear, however this complex have been found to be stimulated to hydrolyse ATP both by DNA and nucleosome.

Binding of the complex to DNA and nucleosome

In order to remodel chromatin, remodeling complexes have to be able to recognize and bind to their substrate. The SWI/SNF complex binds to DNA and nucleosome with high affinity. Snf2p can bind to naked DNA in an ATP-independent manner with K_d in nanomolar range and electron spectroscopic imaging studies have shown that Snf2p binding creates loops in either nucleosomal arrays or naked DNA(4) bringing distant sites into close proximity(4). The binding of the complex seems to occur through the minor groove of DNA as the complex is displaced by distamycin A or chromomycin A3, which are minor groove binding agent(47). The DNA-binding properties of the ySWI/SNF complex are similar to those of HMG box proteins, which bind nonspecifically to DNA in a length-dependent manner with a preference for four-way junctions(60). Extensive studies have not been able to demonstrate any DNA sequence specificity for the SWI/SNF complex. The affinity of Snf2p for nucleosomes is slightly higher than that for naked DNA. This is possibly due to additional interactions of the protein with the acetylated histones through the bromodomain(15). Depletion of the H2A/H2B dimer either *in vivo* (by mutations) or *in vitro* (by addition of H2A/H2B chaperones) has been demonstrated to bypass SWI/SNF requirements. In contrast, human SWI/SNF (hSWI/SNF) is able to remodel tail-less mononucleosomes, as well as

nucleosomal arrays, suggesting that the mechanism of nucleosome remodeling by hSWI/SNF is not dependent on the core histone tails (26).

ATP-dependent nucleosome disruption

In contrast to the DNA binding properties of the complex, which is ATP-independent, the nucleosome remodeling activity of the SWI/SNF is ATP-dependent. This activity of the complex has been observed by two types of experiments. Initially, in assays containing purified SWI/SNF, ATP and nucleosomes, this activity was observed as increased DNaseI sensitivity of the nucleosomal DNA(16). More recently, studies of human SWI/SNF (SWI/SNF) and *S. cerevisiae* RSC have demonstrated that the remodeled nucleosome is stable in the absence of the remodeling complex and has the size of two nucleosomes (15, 29). It is not yet clear if the remodeled nucleosomes observed in the earlier and later assays are the same as each other, as they display some differences in nuclease sensitivity. In addition, both SWI/SNF and RSC can act on the remodeled nucleosome to restore it to the original, inactive, nucleosomal state. While SWI/SNF acts catalytically on nucleosome arrays to form the active state, the properties of the reverse remodeling reaction remain to be characterized.(60).

Biochemical studies show that the SWI/SNF protein complexes can remodel nucleosomes in an ATP-dependent fashion by two mechanisms. The SWI/SNF protein complex can transfer histone octamers to other DNA molecule (*trans*-displacement).(39) And it can also slide histone octamers on the same DNA molecules (*cis*-displacement)(63)(Fig.3). The preference for *cis*- or *trans*-displacement of nucleosomes depends upon the ratio of SWI/SNF complex to the octamer. The complex can catalyze *cis*-displacement quite efficiently even at a low SWI/SNF complex :octamer ratio (one

SWI/SNF complex per 200 nucleosomes), whereas *trans*-displacement requires a tenfold greater SWI/SNF complex:octamer ratio(39).

During the past years, the models for nucleosome mobility have been refined. Chromatin fluidity characterized by more or less random, short-range, ATP-dependent nucleosome movements, provides an elegant solution to the problem of how to maintain the overall packaging of DNA while ensuring that DNA sequences can be accessed by pioneer proteins within a given time frame. Interactions of nucleosome remodeling factors with nucleosomal DNA and particularly with DNA at the edge of the nucleosome have been detected. A selection of potential mechanisms has been considered with two emerging as favourites: Twist defect diffusion and Bulge diffusion(5, 22).

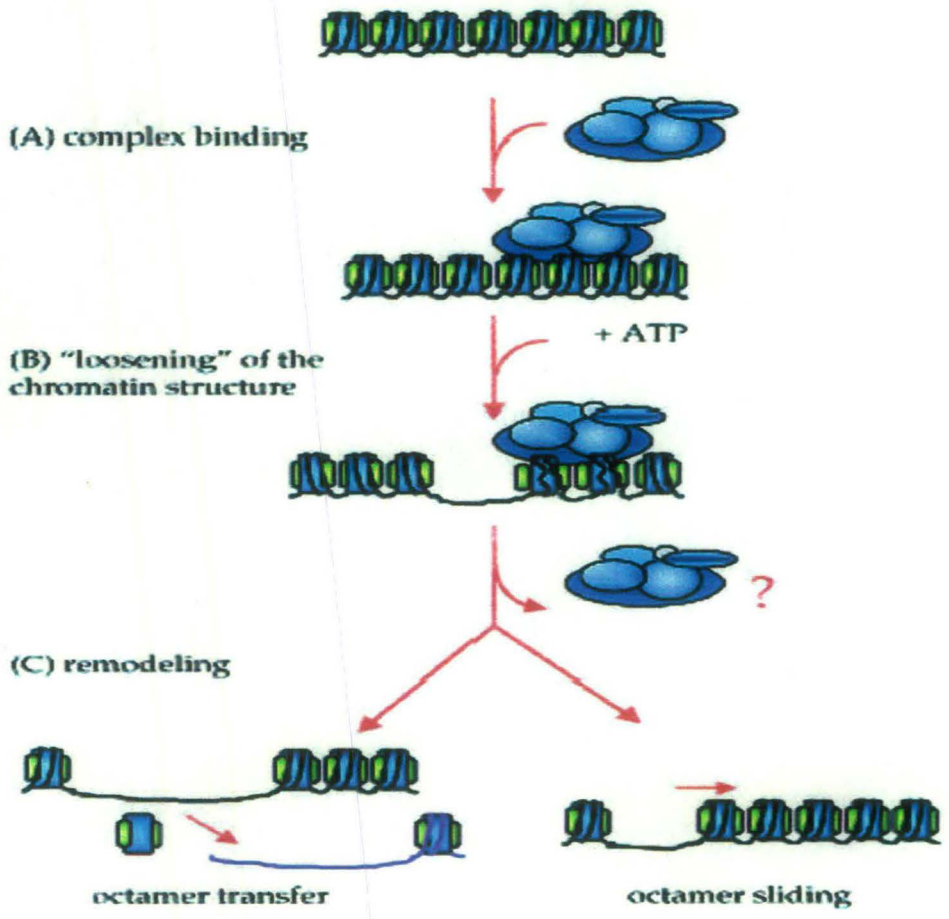

Figure 3: Two-step model of SWI/SNF and RSC action in chromatin remodeling. The binding of the remodeling complex to chromatin is ATP independent (a). Upon ATP addition, the conformation of nucleosomes changes as a consequence of the alteration of histone-DNA interactions (b). This disruption results in remodeling of the chromatin (c), which might occur while the complex is still bound might persist after it is released from the chromatin (indicated by the question mark). Remodeling that occurs may result in transfer of histone octamers to different DNA segments in *trans* or in sliding of the octamers in *cis* (i.e., to a different position in the same DNA molecule). The exact consequence of remodeling is likely dependent on the exact context of nucleosomes at a given promoter and can lead to either (i) activation of transcription or (ii) repression(60).

Twist defect diffusion

In this model, small local alterations from mean DNA twist ('defects') propagate around the nucleosome (Fig 4a). According to this model, histone-DNA interactions at the nucleosomal entry sites may be disrupted by the energy-consuming (un)twisting of DNA in a small domain, presumed to be topologically constrained by the remodeling enzyme itself and the nucleosome substrate. The distortion of DNA may be propagated over the surface of the histone octamer until it emerges on the other side, at which time the histone octamer has relocated nucleosome core particle. Crystal structures give direct evidence for the expected intermediates of twist defect diffusion. Co-crystallisation of nucleosome cores with different DNA sequences or with minor groove binding polyamides demonstrates that the location of these defects can be manipulated(22) (49).

Because remodeling enzymes can alter superhelical torsion within DNA fragments, it is possible they could accelerate the rate of twist defect diffusion. To test the consequence of blocking such torsion, nicks or flaps have been introduced within nucleosomes. Although these did not have substantial effects, interpretation of these experiments is complicated and it is not possible to rule out a role for twist defect diffusion in either thermal or ATP-driven nucleosome redistribution.

Bulge diffusion

In the bulge diffusion model, unpeeling of DNA from the histone octamer at the entry/exit of the nucleosome and subsequent rebinding of more distal sequences to the same histone contact points would establish nucleosomal particles harbouring excess DNA. This is imagined to be looped out in a 'bulge' (Fig 4b). Subsequent migration of the bulge around the nucleosomal superhelix would result in the nucleosome apparently

stepping in the direction where the bulge had initiated. On the basis of the physical properties of DNA, two reports have estimated that large bulges involving the incorporation of at least 40–60 bp of additional DNA into nucleosomes would be most favored. Several recent observations of nucleosome sliding both *in vitro* and *in vivo* are consistent with movements on this scale. However, other explanations are also possible. An alternative approach has been to probe for nucleosome-like structures containing >147 bp of DNA as the predicted intermediates in this mechanism. Two recent reports have provided some support for this(20, 31)

Despite observations consistent with both the twist defect and bulge diffusion mechanisms, further work is required to establish which predominates.

In vitro studies have shown that the ySWI/SNF and hSWI/SNF complexes disrupt the rotational phasing of DNA on the surface of the histone octamer (16). In other words, the complex alters the histone-DNA contacts in an ATP-dependent manner, resulting in a pattern of DNase I digestion different from that of nucleosomal DNA. Another consequence of this disruption is that it enhances the access of DNA-binding proteins to nucleosomal DNA. This has been shown with several types of sequence specific DNA-binding proteins and with restriction endonucleases(34). Mutations in the ATP-binding domain of the Snf2p subunit abolish SWI/SNF activity in these assays(16).

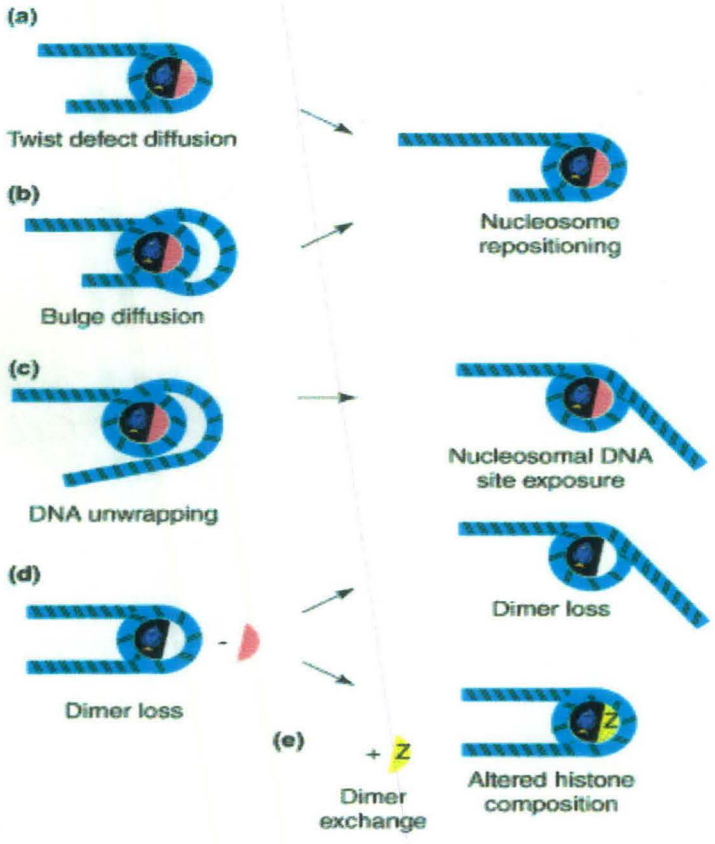

Figure 4: Consequences of histone dimer removal. Two widely favoured but hypothetical actions of remodellers are **(a)** to stimulate diffusion of twist defects around the surface of the nucleosome, or **(b)** to catalyse DNA unwrapping from the nucleosome surface. Twist and bulge diffusion could result in nucleosome repositioning and the exposure of previously occluded DNA sequences as could site exposure **(c)**. The loss of dimers from nucleosomes also occurs during some remodelling reactions **(d)** and if a different histone dimer, for example containing H2A.Z, rebinds this will result in alteration of the nucleosomal histone composition **(e)**(22).

Crystal structure of the ATPase motor domain.

Recently, crystal structure of ATPase motor domain of zebra fish Rad54 and SWI/SNF ATPase core of *Sulfobolus solfataricus* (SSO1653) protein have been determined(18, 56). According to these studies the motor domain is a bi-lobed structure separated by a deep cleft. Each lobe is called as the RecA-like domain and their arrangement is similar as found in helicases(56). Motifs I, II and III are present in domain 1 and motifs IV, V and VI are present in the domain 2. Motifs I, II and III from domain 1 form the ATP-binding site in the active site cleft. Motifs IV, V and VI on domain 2 are not situated in the active site cleft in case of SSO1653, but position on the outside of the protein. This unique location is due to the -180° degree flip of the domain 2, which is very unusual in case of helicases(18). Besides, the helicase core structure, the Snf family structures haves some additional structural element inserted into the helicase core. These comprise the antiparallel alpha helical protrusions from both recA-like domains 1 and 2, a structured linker between the recA-like domains; the major insertion region at the back side of the domain 2 alpha helical protrusions and a triangular brace packed against the domain 2 alpha helical protrusions. The two alpha-helical protrusions and linker are all encoded within the enlarged span between motifs III and IV. The triangular brace is encoded immediately downstream of motif VI (Fig. 5).

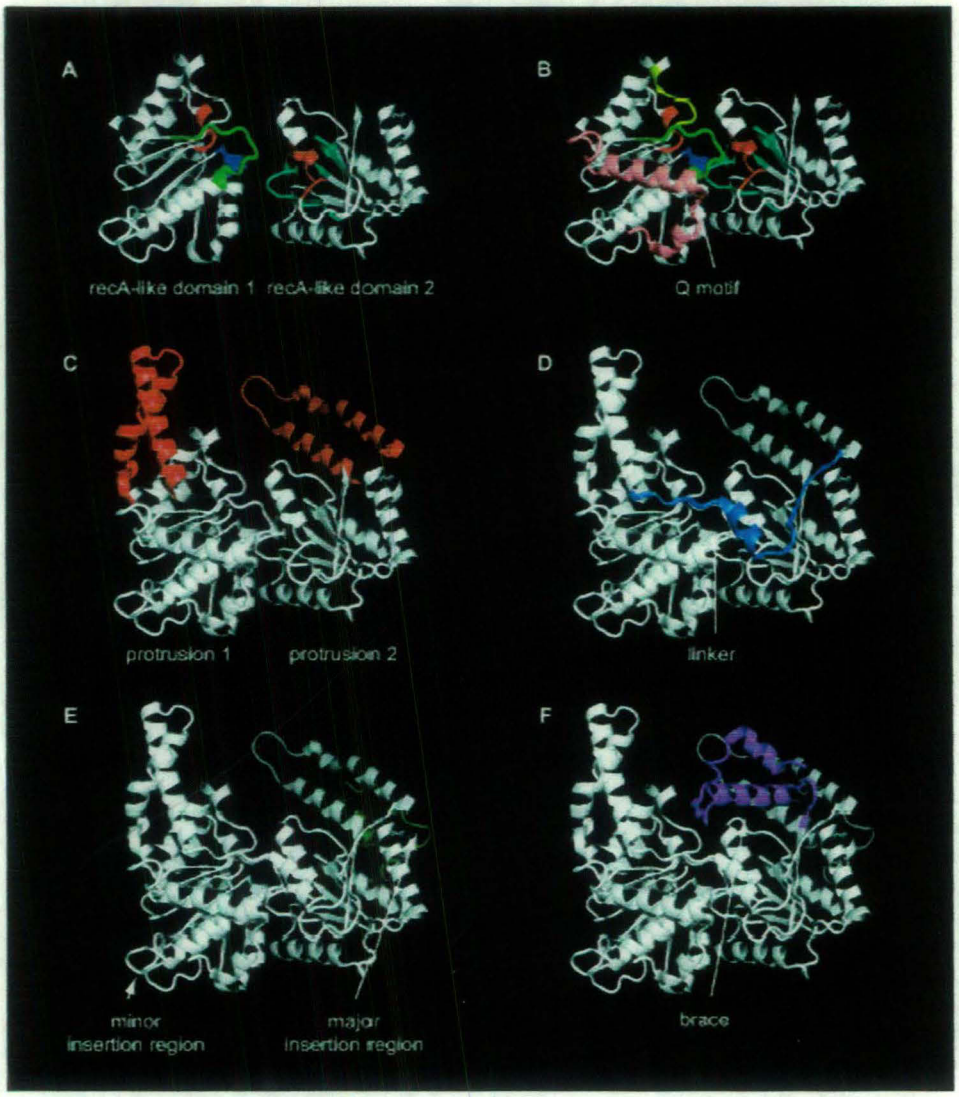

Figure 5: Conserved blocks contribute to distinctive structural features of Snf2 family proteins. (A) core recA-like domains 1 and 2 including colouring of helicase motifs (I in green, Ia in blue, II in bright red, III in yellow, IV in cyan, V in teal and VI in dark red). (B) Q motif (pink). (C) antiparallel alpha helical protrusions 1 and 2 (red) projecting from recA-like domains 1 and 2, respectively. (D) Linker spanning from protrusion 1 to protrusion 2 (middle blue). (E) Major insertion region behind protrusion 2 (light green). (F) triangular brace (magenta).(21)

The structure and sequence of Motif I (ATP binding) and Motif II ($MgCl_2$ binding) between Rad54 and other helicase are highly similar. The sequence of the remaining motif in domain 1 (Ia,TxGx and III) are different from those in SF1/SF2 helicases but the structure suggest that these motif overall have the similar function in Rad 54. Comparison between the structure of the SF1/SF2 helicases and Rad54 show that Ia and TxGx may be involved in DNA binding. Motif III of Rad54 has sequence and structural similarity with the SF2 helicase, but contains some additional residues in SWI/SNF proteins. In helicases, Motif III interacts with the gamma phosphate of ATP, DNA and the second domain. This motif has been suggested to be a sensor for ATP hydrolysis. The domain 2 contains a DNA binding motif (Motif IV) that is structurally conserved in SF1/SF2 helicase and Rad54. In helicases, the motif IV interacts with DNA through one or two basic residue, as well as through the amide back bone group at the start of the helix. Rad 54 and the remainder of the SWI/SNF do not have the basic residue seen in helicases. However, Rad54 has a lysine 449 residue at similar position as that present in helicases. Thus, Lys449 not only provides potential DNA contact that is otherwise absent in Motif IV but also provides a mechanism for involving domain 2 in DNA binding. Rad54 and other SWI/SNF protein have a conserved Arg/Lys,(Lys568), Ser/Thr Ser(566), and Ser(567), and Gly(570) in the motif V that might interact with DNA in a manner analogous to PcrA and Rep(56). Motif VI in Rad54 and other SWI/SNF protein have a conserved arginine. In crystal structure, Arg 600 interacts with sulfate ion bound in the ATP gamma phosphate binding site of motif I in a manner analogous to that seen in PcrA(18). Crystal structure studies of SSO1653 shows that DNA binds predominantly to subdomain 1A by recognition of the two phosphate chains

along the minor groove. The Ia and II region were found to be involved in DNA binding. Arg547, a highly conserve residue of the SWI/SNF in the Ic motif, was found to interact with the minor groove of the DNA. Domain 2 binds to the DNA -phosphate backbone through Arg728 and Lys781. This binding is much weaker as compared to the interaction with the domain 1. The DNA binding constant of catalytic domain of SsoRad54(SsoRad54cd) as a whole is 0.1+/- 0.02μM for dsDNA and 11+/-5 μM; domain 1 by itself has reduced binding activity 0.2+/-0.1 compared to full length protein, whereas domain 2 does show any DNA binding activity at all. DNA binding of SsoRad54cd is not significantly affected by the ATP or non-hydrolysable ATP analogs (18). Comparative studies of SsoRad54 and Rad 54 with DNA helicase PcrA and RNA helicase NS3 shows that RecA-like fold and location of motif I-III is preserved between the enzymes(56). PcrA and NS3 have single strand binding domain which firmly grabs the base of the single strand. SsoRad54cd was found to lack the ssDNA binding domain but it can bind to 5'-3' DNA through domain 1. Similarly, Rad54 was able to bind to DNA through domain1. SsoRad54cd lacks ssDNA binding domain and hence they do not have ssDNA- stimulated ATP hydrolysis activity, which may suggest that it cannot translocate ssDNA in ATP hydrolysis dependent manner. Crystallographic studies show that the DNA is fully base-paired along the entire side of SsoRas54cd and there is no upstream helix destabilizing region. This may explain why SWI/SNF proteins do not have helicase activity.

DNA-dependent ATPAse A

DNA-dependent ATPase A is a member of the SWI/SNF protein family. This protein possesses the seven helicase domains which are characteristic of the SWI/SNF family members. The human homolog is known as SMARCAL1. Recently, this protein has been grouped into SMARCAL1 subfamily(21). This subfamily consist of human SMARCAL1 (SMARCA-Like 1) and its homologue HARP.

DNA-dependent ATPase A was first isolated as a 105-kDa protein from calf thymus and Northern blot analysis has confirmed the presence of mRNA corresponding to that gene in bovine system(42). Southern Blot analysis has shown the presence of the gene in multiple copies in human, bovine and murine tissue. The protein has DNA-dependent ATP hydrolysis in presence of a DNA effector(44). This protein has been found to undergo proteolytic cleavage resulting into two polypeptide of molecular masses 68-kDa and 82-kDa.

The 82-kDa polypeptide lacks the N-terminal sequence but retains all the seven helicase motifs and it also has DNA-dependent 24.8 μmol of ATP hydrolyzed / min/ mg of protein) even though it less as compared to the 105-kDa(171 μmol ATP hydrolyzed /min/mg). The 82-kDa is called as the **Active DNA-Dependent ATPase A (ADAAD)** and this domain contains the motor domain of SWI/SNF family. Clustal W analysis hsve shown that this protein have all the seven conserved domain found in other member of the SWI/SNF family (Fig. 6)

```
                                                                I
scRad           DEAEYSQDISFTEQNNRGAYGCIMADEMGLGKTLQCIALMWTLKLIDKCIIVCPSSLVNN
hRad54          QECFLPFRKPLIP----GSHGCIMADEMGLGKTLQCITLMWTLKEIDKAVVVSPSSLVKN
hERCC6          PVQETPFGTQILWELHCQQAGGILGDEMGLGKTIQIIAFLAGLRGLGPTVIVCPTTVMHQ
scSNF2          NSQTVEENETIMVSLFNNHLNGILADEMGLGKTIQTISLLTYLKIRGPYLVIVPLSTLSN
scSth1          ESKFSALGDPDMVSLYNNHLNGILADEMGLGKTIQSISLITYLKDIGPFLVIVPLSTITN
hSmarcal        KPKSSRDAKLEVNFAIAKGGRLLLADDMGLGKTIQAICIAAFY-KEWPLLVVVPSSVRFT
bSmarcal1       KVKNFRDPELEVNFAIAQRGRLLLADDMGLGKTIQAICIAAYY-KEWPLLVVVPSSVRFT
                                  ::.*:******:* * :          ::: * :
                      Ia
scRad           WANELIKWLGPNTLTPLAVDGAIHAWAQAQGRNIVKPVLIISYETLRRNVDQLKNCNVGL
hRad54          WYNEVGKWLG-GRIQPLAIDGKLEGFMNQRGARVSSPILIISYETFRLHVGVLQKGSVGL
hERCC6          WVKEFHTWWPPFRVAILHETGTHKKEKLIRDVAHCHGILITSYSYIRLMQDDISRYDWHY
scSNF2          WSSEFAKWAP--TLRTISFKGNERKAKQAKIRAGEFDVVLTTFEYIIKERALLSKVKWVH
scSth1          WTLEFEKWAP--SLTTIIYKGNQRHSLQHQIRVGNFDVLLTTYEYIIKDKSLLSKHDWAH
hSmarcal        IEQIFL WLP--SLSIDCIN----VVTG D LTIGLINISFDLLS LE QL T-FF
bSmarcal1       WEQAFCRWLP--SLNPLDINV----VVTGKDRLTDGLVNIVSFDLLSKLEKQLKP-PFKV
                *   .  *     :                :       : : ::. :       :.
                      II                              III
scRad           MLADEGHRLKNGD-SLTFTALDSISCPRRVILS-GTPIQNDLSEYFALLSFSNPGLLGSR
hRad54          VICDEGHRLKNSE-NQTYQALDSLNTSRRVLIS-GTPIQNDLLEYFSLVHFVNSGILGTA
hERCC6          VILDEGHKIRNPN-AAVTLACKQFRTPHRIILS-GSPMQNNLRELWSLFDFIFPGKLGTL
scSNF2          MIIDEGHRMKNAQSKLSLTLNTHYHADYRLILT-GTPLQNNLPELWALLNFVLPKIFNSV
scSth1          MIIDEGHRMKNAQSKLSFTISHYYRTRNRLILT-GTPIQNNLPELWALLNFVLPKIFNSA
hSmarcal          IIDESHFL NS TI C IIIIFVL VL  IILLSGTPAMS PAELYTQILAV PTFFPQF
bSmarcal1       VIIDESHFLKNIKTAVC-AAMPLLKVAKRVILLSGTPAMSRPAELYTQILAVRPTFFPQF
                :: **.* ::*                  *:::  *:*  .   * :: .    .  :

scRad           AEFRKNFENPILRGRDADATDKEITKGEAQLQKLSTIVSKFIIRRTNDILAK--YLPCKY
hRad54          HEFKKHFELPILKGRDAAASEADRQLGEERLRELTSIVNRCLIRRTSDILSK--YLPVKI
hERCC6          PVFMEQFSVPITMGGYSNASPVQVKTAYKCACVLRDTINPYLLRRMKSDVKMSLSLPDKN
scSNF2          KSFDEWFNTPFANTGGQDKIELSEEETLLVIRRLHKVLRPFLLRRLKKDVEK--ELPDKV
scSth1          KTFEDWFNTPFANTGTQEKLELTEEETLLIIRRLHKVLRPFLLRRLKKEVEK--DLPDKV
hSmarcal        HIIGL YCDA  IFIGADYSGSSNLGEL LL-----LEEAVMLRRLKGDVLS--QLPAKQ
bSmarcal1       HAFGLRYCGAKRQPWGWDYSGSSNLGELKLL-----LEEAVMLRRLKGDVLS--QLPAKQ
                  *   :  .                                  ::** .  :     ** *

scRad           EHVIFVNLKPLQNELYNKLIKSRE-VKKVVKLKKLCNHPNLLNFKFSILERFLHKIKTES
hRad54          EQVVCCRLTPLQTELYKRFLRQAKPAEELLELKKLCNHP-ALIYKMLVLDYILAVTRSRS
hERCC6          EQVLFCRLTDEQHKVYQNFVDSKEVYRILNG--KICNHPDLFSGKMIVVESLLKIWHKQG
scSNF2          EKVVKCKMSALQQIMYQQMLKYRRLFIGDQNLKKICNHP--FVFKFELLDRILPKLKATG
scSth1          EKVIKCKLSGLQQQILYQQMLKHNALFVGAGTLKKICNHP--FVFKFELLDRVLPKFKASG
hSmarcal          IVVIAFG INA T AALDIAA EMTT D - QQQ DALILFF IFSIIEYILDLLESG
bSmarcal1       PRWWWSPQARSMPGPEPPWMPPAKEMTTKDK-KQQQKEALILFFKIPSIIEYILDLLESG
                 :                                  :  :..  :  *:  :   :      .
                          IV
scRad           DDKIVLISNYTQTLDLIEKMCRYKHYSAVRLDGTMSINKRQKLVDRFNDPEGQEFIFLLS
hRad54          SDKVVLVSNYTQTLDLFEKLCRARRYLYVRLDGTMSIKKRAKVVERFNSPSSPDFVFMLS
hERCC6          -QRVLLFSQSRQMLDILEVFLRAQKYTYLRMDGTTTIASRQPLITRYN-EDTSIFVFLLT
scSNF2          -HRVLIFFQMTQIMDIMEDFLRYINIKYLRLDGHTKSDERSELLRLFNAPDSEYLCFILS
scSth1          -HRVLMFFQMTQVMDIMEDFLRMKDIKYMRLDGSTKTEERTEMLNAFNAPDSDYFCFLLS
hSmarcal          E FLIFAHH VVLDAITQELE H QH  IDGSTSSAE EDLCQQFQL-SE HAVAVLS
bSmarcal1       REKFLVFAHHKVVLDAITKELERKRVQHIRIDGSTSSADRETSASSFS--CPRALRGVLS
                 .:.::. :    :* :    .      :::**  .  .*       :.         :*:
```

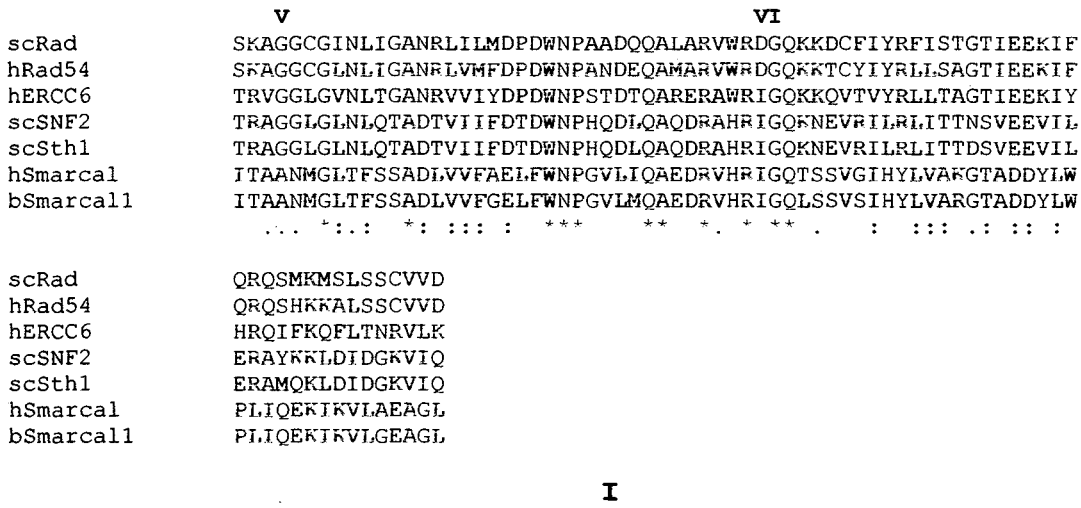

Figure 6: Clustal W of FLADAAD with other member of the SWI/SNF family

The cDNA of this protein has been cloned and expressed in *E. coli*. The ATPase activity and other relative effector recognition of ADAAD are similar to the parent protein(44). Studies with ADAAD have shown that it has preference for some particular structure of the DNA. The ability of ADAAD to interact with these different structures of DNA was measured as a function of ATP hydrolysis. Stem-loop DNA containing a 13 base loop and a 12 base-pair stem was found to be the optimal effector for ADAAD. DNA molecules that possess the character necessary to yield a double-stranded to single-stranded transition region, such as mismatches of 4 and 10 base pairs or AT-rich sequence, were found to be effectors of ADAAD. Single-stranded DNA molecule, double-stranded, and blunt-ended DNA was not capable of effecting ATP hydrolysis by ADAA. ATP hydrolysis was also hydrolysed differentially in presence of DNA having 3'- and 5'-recessed termini. ATP hydrolysis was found to be preferentially effected by DNA molecules with a double-stranded to single-stranded transition and a 3'-hydroxyl terminus in close proximity to the duplex region (44).

Role of the helicase motifs

Studies carried out with other related protein like helicases and some of SWI/SNF motor domain having these motifs have shown that the Motif I is a conserved GKT sequence (Walker A box) which is found in most nucleotide binding proteins(61). The Motif II overlaps with the DEAD box (DE-is highly conserved), a special version of the Walker B motif of nucleotide binding proteins(38). Motif Ia and a conserved tyrosine within Motif VI have been associated with presume DNA binding protein, suggesting an involvement of the sites for polynucleotide binding. A conserved aspartate residue in motif II has been implicated in phosphate binding via magnesium ions. Motif III has sequence homology to viral DNA polymerase. The role of the Motif V and VI have not yet been found.

Human SMARCAL1

ATP-dependent chromatin remodeling complex contain several sub unit, one which is a SWI/SNF related ATPase domain. The ATPase domain is very important for the complex as it is involved in ATP hydrolysis, which is required for carrying the remodeling processes. Also these proteins interact with others protein in the complex both through their C-terminal and N-terminal region. Mutation in SMARCAL1 which is a human homolog of ADAAD is responsible for the autosomal recessive diseases called Schimke Immuno-Osseous Dysplasia(SIOD)(6). Mutation in this gene leads to pleitropic disorder like spondyloepiphyseal dysplasia, renal dysfunction and T-cell immunodeficiency. The involvement of SMARCAL 1 in SIOD was determined using genome-wide linkage mapping and a positional candidate approach. Most of the missense

mutation that are associated with the disease, lies in the SNF2 domain and alters some of the residue which are conserved in human ,mouse, *D. melanogaster* and *Caenorhabtidis elegans,* which are presumably very crucial for SMARCAL1 function. The severity on the disease depends on the type of mutations in the gene of SMARCAL1. R561C missense mutation causes a milder type of SIOD(7). Mutations in the conserved arginine residues were found to be more common in SIOD. Also some of the mutations were found to be occurring in the ATP and DNA binding region of the SNF proteins. Similarly, BRG1 and hBRM which are ATPase domain found in human SWI/SNF complex are found to be mutated in many cancers(48). ADAAD which is a bovine homolog of SMARCAL 1 can be use as a model to understand how those motifs in the SNF domain function and also we will try to delineate the function of each of the conserved residue.

Hypothesis

Crystal structure studies of the ATPase motor domain of Rad54 demonstrate that the protein possess a bi-lobed structure with two domains separated by a cleft or a hinge region. DNA binds to the protein through this cleft. These studies also demonstrate the the possible involvement of these different motifs in DNA binding and ATP binding (18, 56).

We propose that the cleft provides the basis for the DNA-dependent ATP hydrolysis that is observed in SMARCAL1. In the absence of DNA, the protein conformation is such that ATP, even if it binds through the Motif I and II, can not be hydrolyzed. When DNA binds through the cleft, the protein undergoes a conformation that results in ATP hydrolysis.

Scope of the work

To test our hypothesis, we are trying to elucidate the significance of each of the two domains in ADAAD and their role in ATP and DNA binding by constructing deletion mutants Also, ADAAD have tryptophan residue in the Ia region which is conserved in most SWI/SNF protein. These residues which are conserved may have a role in ATP and DNA binding. As we know that tryptophan residues are mainly responsible for the fluorescence of proteins, the role of these tryptophan residues in the ATP and DNA binding can be monitored by observing the change in fluorescence. Comparative study will be done for the mutant and the wild type protein with respect to DNA binding and ATP binding. In this study we are trying to study the binding constant of the wild type protein and mutant to DNA and ATP using fluorescence spectroscopy.

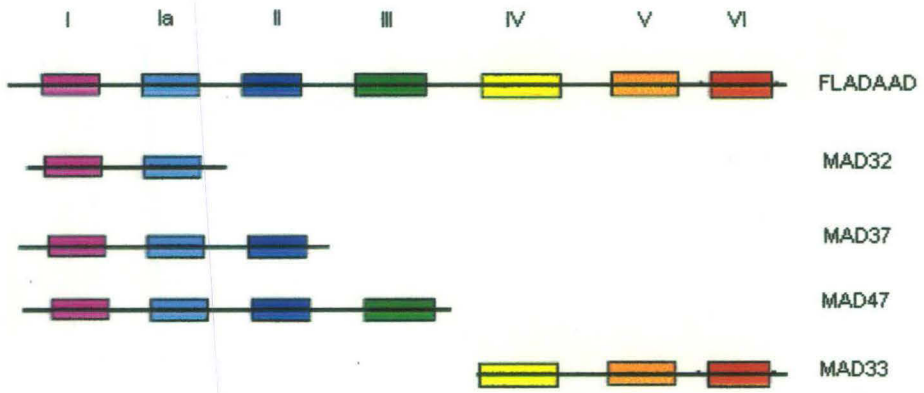

Figure 7: Different deletion mutant of FLADAAD

MATERIALS AND METHODS

Buffer Compositions

All the buffer compositions are provided in the appendix.

Strains

The bacterial strains DH5α (BangaloreGenei) and DH10B were used for cloning purpose. BL21 (DE3) cells were used for expression studies. DH10B and BL21 (DE3) were kind gifts from Dr. Suman Dhar, Special Center for Molecular Medicine, Jawaharlal Nehru University.

Chemicals

All chemical were of analytical grade and were purchased from Qualigen (India), SRL (India), Merck (India), Sigma-Aldrich (USA), or Amersham BioSciences (USA). Restriction enzymes and T4 DNA ligase were purchased from MBI Fermentas (USA), New England Biolabs (USA), and Bangalore Genei (India). TA cloning kit was obtained from Qiagen (USA), and from MBI Fermentas (USA). Gel extraction kit and plasmid extraction kit were purchased from Mdi Advanced Microdevices Pvt Ltd. (India). Bradford dye for protein estimation was purchased from Sigma-Aldrich (USA). Glutathione beads were obtained from Genotech Bioscience (USA). pCP101, which contains His-tagged ADAAD, was a kind gift from Dr Joel W.Hockensmith, University of Virginia.

Vectors

pGEX-6P-2 (Amersham) was a kind gift from Dr Suman Dhar, Special Center for Molecular Medicine, Jawaharlal Nehru Univertsity.

Primers

The primers for amplification of FLADAAD were designed using the primer design software available on Saccharomyces Genome Database (http://seq.yeastgenome.org/cgi-bin/web-primer). The primers for FLADAAD were synthesized by MWG-Biotech AG and BioServe India. The sequences of the primers are:

Forward primer 5'**GAATTC**GC**CATATG**GCAGGGACCCCGATGCACA 3'

Reverse primer 5' **CTCGAG**TTATAGAGGAGAGGTAAAGC 3'

The forward primer carries the EcoRI and NdeI restriction site. The reverse primer carries XhoI restriction site, allowing for cloning into multiple cloning site of pGEX6p-2 vector. The same primers were used for amplifying MAD37.

DNA effector for ATPase assays:

We have used a stem-loop DNA for ATPase studies as this has been previously determined to be the most effective effector for ADAAD.

Stem-loop DNA: 5'GCGCAATTGCGCTCGACGATTTTTTAGCGCAATTGCGC 3'

Cloning of FLADAAD and MAD37 into expression vector

PCR amplification

For cloning of FLADAAD into expression vector, PCR amplification of the gene was done. The gene was amplified using pCP101 as the template. The PCR reaction mixture contains 0.2 μM dNTP's, 200μM each of the primer, 1X Taq buffer and 1 unit Taq polymearse (25μl reaction). Different concentrations of $MgCl_2$ (0.5mM to 3.5mM) were used for optimizing amplification. PCR was also carried out using Pfu

polymerase and in this case different concentrations of $MgSO_4$ from 0.5mM to 1.5mM were used. However, the concentration of primers and dNTP's were not changed. Similarly, for cloning of MAD37 the above conditions was followed using the same primers that were used for cloning ADAAD except that the template used is pRM102. The PCR conditions are given in Table (2a and 2b)

Table 2: PCR conditions for a) FLADAAD b) MAD37

a)

94°C	5mins
94°C	45sec
56°C	30sec
72°C	2min
72°C	10min
For 30 cycles	

b)

94°C	5mins
94°C	45secs
56°C	30secs
72°C	1.5mins
72°C	10mins
For 30 cycles	

Purification of the PCR amplicons

The amplicons were extracted from the agarose gel and purified using gel extraction kit (MDI) by following the instructions provided with the kit.

'A' tailing of the PCR amplicons

The 3' end of the Pfu amplified PCR products were tailed with d (A) using Taq polymerase. 1-7µl of the PCR amplicon was mixed with 1 µl Taq polymerase in 10X

buffer having $MgCl_2$. dATP was added to final concentration of 0.2mM in a 10µl reaction volume. The reaction mixture was incubated at 72°C for 30-45 minutes.

Restriction Digestion

pGEX-6P-2 vector was digested using EcoRI and XhoI and the restricted product was purified using gel extraction kit. Similarly, the insert was released from the T/A cloning vector using EcoRI and XhoI and separated using agarose gel electrophoresis. The insert was extracted from the agarose gel using gel purification kit.

Ligation

T/A clone:-The 3'-A tailed PCR amplicons were ligated into pTZ57R/T plasmid. 4µl of the amplicon was taken and incubated with 1µl of the plasmid in presence of T4 DNA ligase in a 10µl reaction. The ligation mix was incubated at 22°C for 16hrs.

Cloning into pGEX-6P-2 vector:-The insert released from T/A vector was ligated into pGEX-6-P2 vector. The ligation reaction was carried out in 10µl reaction using different vector:insert ratios. T4DNA ligase was added and the ligation mix was incubated at 22°C for 16hrs

Transformation

2-4µl of the ligation mix was transformed in to DH5α competent cells and plated on LB agar containing appropriate antibiotics and incubated at 37°C for at least 16 hrs. For expression studies, BL21 (DE3) cells were used.

Selection of Transformants

The colonies, which grew on the plate, were picked up and streaked in another fresh LB-ampicillin plate and incubated for 16 hrs. Colony PCR was done with these colonies to check the present of insert. The PCR positive clones were subsequently crosschecked by restriction digestion. Finally, the presence of insert was confirmed by sequencing.

The vector pGEX-6P-2 carrying the insert of FLADAAD was named pMN82 and pGEX-6P-2 vector carrying the insert of MAD37 was named pMN37

Plasmid Extraction

The clones were grown overnight in 10mL culture at 37°C in presence of 100μg/mL ampicillin. Plasmid extraction was carried out by alkaline lysis method as described in Molecular Cloning manual

Expression of FLADAAD and MAD37

The pMN82 and pMN37 plasmids were transformed into BL21 (DE3). The cells carrying the respective plasmids were set up for primary culture by inoculating a single colony into LB media having 100μg/ml ampicillin. The cells were incubated at 37°C in a shaker incubator. Secondary culture was set up by adding 1% inoculum from the primary culture into fresh medium having 100μg/ml ampicillin. Cells were grown at 37°C till OD reached 0.5 at 600nm. Cells were induced at this OD with 0.5mM IPTG. After induction the cell were grown for a further period of 4 hrs and then harvested by centrifuging at 5000 rpm. Supernatant was discarded and 1X PBS was added to the pellet and processed

further for SDS-PAGE. Expression studies were also carried out by inducing cell at different temperatures, IPTG concentrations, and time.

SDS-PAGE:

10% and 8% resolving gel with 5% stacking gel were used for analyzing the expression pattern of the proteins(50). The samples were mixed with gel loading dye boiled for 5 min and loaded onto the gel. Equal number of cells as calculated by OD_{600nm} measurement was loaded onto the gel.

Rf calculation:

The size of the protein was calculated by measuring the Rf of the protein .A graph between Log Molecular weight and Rf of the protein was plotted.

Solubilisation studies

Solubilisation of protein was done by inducing at different temperature, IPTG concentrations and using different lysis buffers. The cells were incubated with lysis buffer for 1 hour at 4 °C on a rocker. After incubating with lysis buffer the cell were sonicated for 10 cycles (15seconds on/45 seconds off) using ultrasonicator. The soluble fraction was separated from the insoluble fraction by centrifuging the cell at 12000rpm for 30 minutes in Sorvall centrifuge. Supernatant and pellet were analysed by SDS PAGE to check the solubility of the protein.

Bead Assay:

Before going for large scale purification of the proteins, a small bead assay was performed to check the binding of the protein to Glutathione bead and also to standardize the purification protocol. 50 ml secondary culture was grown at 25°C for 4 hours for MAD 37 and 16°C overnight for FLADAAD. After solubilisation of the protein, 1.5ml

of the supernatant was incubated with 150µl Glutathione bead, pre-equilibrated in equilibration buffer, for 1 hour at 4°C. After incubation the beads were harvested by centrifuging at 2500 rpm for 5 minutes. The supernatant was removed and the beads are washed with wash buffers having different salt concentrations (150mM-500mM NaCl). Washing was done by rocking the beads with the wash buffer at 4°C for 10-15 minutes. After each washing the beads were harvested by centrifuging at 2500 rpm for 5 minutes. Finally, the beads were incubated with elution buffer containing glutathione for 1 hour to elute the protein. Elution buffers having different salt concentrations and different incubation periods were also used to optimized the elution of protein.

Large scale purification of MAD37 and FLADAAD

For purification of the proteins 1L culture of cell was grown in a shaker incubator at 37°C, till OD_{600nm} reached 0.5. Cells were shifted at 16°C till OD_{600nm} reached 0.8. Cells were induced using 0.25mM IPTG for 16hrs. Cells were then harvested by centrifuging at 8000 rpm for 5 minutes at 4°C. 4.5 gm of pellet was resuspended in15 ml lysis buffer 6 and incubated on a rocker platform at 4°C for 1hr. The cells were sonicated for 10 times (15seconds on/45second off) and the cell debris was separated by centrifuging at 12,000rpm for 30 minutes at 4°C in a Sorvall centrifuge. 1ml of Glutathione bead, pre-equilibrated with equilibration buffer was mixed with the supernatant for 1hr at 4°C. The beads were then loaded onto a column and washed with 10 column volumes of wash buffer. Protein was eluted by using elution buffer containing 50mM Tris-Cl pH 8.0, 100mM NaCl, 25% (v/v) Glycerol, 5mM β-mercaptoethanol and

10mM reduced Glutathione. 250 µl fractions were collected through the entire procedure for further analysis.

Protein estimation

Protein estimation was done using Bradford reagent(8). Reactions were carried out in a microtiter plate according to the protocol provided with the reagent. Reading was done using Spectromax microplate reader (MTX Lab Systems, Inc, USA) at 655 nm.

ATPase Assay

ATPase assay was done using a modification of King's method(32). ATPase assay was done by incubating 3.2µg protein with REG buffer containing 50mMTrisSO_4, 5mM β-mercaptoethanol, 1mM $MgSO_4$, 150µg/ml Pyruvate kinase and 10mM phosphoenolpyruvate. ATP was added to a final concentration of 2mM and stem-loop DNA was added to final concentration of 10nM. The reaction mix was incubated for 1 hr at 37°C. The reaction was stopped by adding solution E and color development was stopped by adding solution F. Reading was done by measuring absorbance at 655nm(23).

Fluorescence Studies

Fluorescence emission intensity measurement was performed with Cary-Varian Spectrofluorometer, USA. Excitation and emission slit width was kept at 5nm each for FLADAAD. In case of MAD37 the emission slit width was kept at 10nm. The proteins were excited at 295 nm and the emission was monitored from 310-400 nm. Change in fluorescence was monitored at 338nm. DNA titration was done by adding 1µl of DNA (stock 500nM) till no change in fluorescence was observed. ATP titration was done by

adding 1µl of ATP (500mM) till no further change in fluorescence was observed. The K_d was calculated using the following equations.

$[P] + [L] \rightleftharpoons [PL]$

[P] is the protein concentration; [L] is the ligand concentration

[PL] is the protein ligand concentration

$K_d = [P][L] / [PL]$, where K_d is the binding constant

When 50% of the binding is complete then [P] = [PL]

Therefore, $K_d = [L]$

On plotting PL vs L the K_d is equal to ligand concentration when half of the protein is bound

The double reciprocal plot linearised this graph to minimize the error.

$K_d = [P][L] / [PL]$

$K_d / [L] = [P] / [PL]$

$y = mx + c$

[P] / [PL] vs 1/ [L]

in terms of fluorescence signal this can be represented as $\Delta F/F_{ini}$ vs 1/[L]

where F_c is the fluorescence intensity which has been corrected for dilution

F_{ini} is the initial fluorescence.

ΔF is $F_c - F_{ini}$

RESULTS

Cloning of FLADAAD

FLADAAD gene, which is 2.2 kb in size, was cloned from pCP101 using gene specific primer in pGEX-6P-2 vector such that a GST-tag will be present at the N-terminus. Proteins inserted into pGEX-6P-2 vector will be expressed as GST tagged protein which will allows us to purify the protein using Glutathione beads. Moreover, the GST tag can be removed later on using PreScission protease.

The primers for the gene carried the EcoRI and XhoI in forward and reverse primer respectively, allowing us to clone into these sites present in the vector. Optimization of PCR condition was done using different concentration of $MgCl_2$. $MgCl_2$ titration was done to check at which concentration amplification was maxmimum. Amplification was seen in all the different concentrations i.e. 1mM, 1.5mM 2.0mM, 2.5mM and 3.5mM of $MgCl_2$. We chose 2 mM $MgCl_2$ for amplification of the gene from pCP101 vector (data not shown). Higher concentrations of $MgCl_2$ were not used since probabilities of errors during amplification are high.

Large scale amplification was done to purify the amplicon using Pfu polymerase from agarose gel using gel extraction kit. Since amplification using Pfu polymerase results in blunt-end products, 'A'- tailing was done at 3'-end, using the method outlined in the *Materials and Methods* section, so that they could be cloned into the T/A cloning vector. The 'A'- tailed amplicons after purification using the gel extraction kit was ligated into the T/A cloning vector. The ligation mix of the T/A vector was transformed into DH5α cells and transformants were selected by colony PCR (Fig.8). The positive

clones were finally confirmed by restriction digestion of the plasmid using EcoR I and Xho I, which resulted in the release of the insert from the vector.

The gene was then released from the T/A clone using EcoRI and XhoI for further cloning purposes (Fig.9). The insert released from T/A vector was ligated into pGEX-6P-2 vector digested with EcoRI and XhoI. The ligation mix was transformed into DH5α competent cells. The transformed cells were screened for the presence of insert by colony PCR (data not shown) and then finally confirmed by restriction digestion (Fig.10)(61). pGEX-6P-2 carrying the insert of ADAAD was named as pMN82 and was transformed into BL21DE3 competent cell for expression studies.

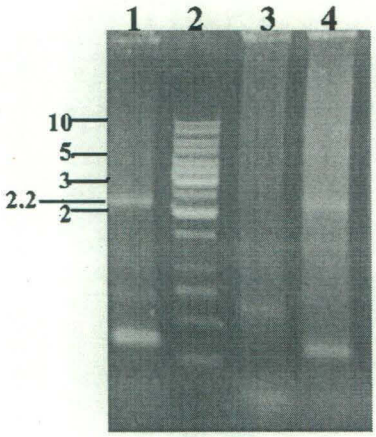

Figure 8: Colony PCR of T/A clones obtained after transformation of the ligated products into DH5α cells. Lanes 1 is a positive control and 4 show the amplification of the expected 2.2 kb product, and thus is PCR positive. Lanes 3 is the negative clone. All the molecular sizes indicated in the figure are in kb.

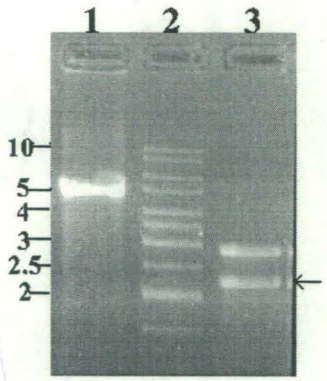

Figure 9: Restriction digestion of T/A clone by EcoRI and Xho I to release the insert. Lane 1 and 3 shows the plasmid linearized with EcoRI and EcoRI-XhoI digested plasmid respectively. Lane 2 is the molecular weight marker. All the molecular sizes indicated in the figure are in kb

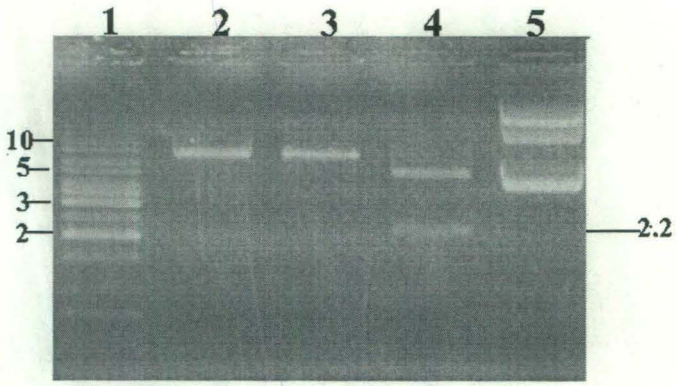

Figure 10: Restriction digestion of pGEX-6P-2 clone by EcoRI and Xho I to release the insert. Lane 2 and 3 shows the linearised plamid cut with EcoRI and Xho I respectively. Lane 4 shows the release of insert from pGEX-6P-2 plasmid after EcoRI-XhoI digestion. Lane 1 is the marker and Lane 5 is the uncut plasmid. All the molecular sizes indicated in the figure are in kb

Cloning of MAD37

MAD37 is a deletion mutant of ADAAD which have first three motif i.e. the GKT box (Walker A), Ia and DESH box (Walker B)(61). The gene for this mutant was obtained by cloning the PCR amplicon amplified from a template pRM102, which has a nucleotide change leading to lysine (334) codon being converted into a stop codon, resulting in a 37-kDa protein containing only motifs I, Ia and II. Therefore, this mutant has only the Walker A and B motifs along with Motif Ia. All these three motifs have

been implicated in ATP-binding and thereby, providing us with a system that would enable us to deduce the role of each of these three motifs in ATP binding and hydrolysis. Cloning strategy similar to FLADAAD was employed to insert this gene into pGEX-6P-2 vector so that the overexpressed protein has a GST-tag at the N-terminus. .

Overexpression of FLADAAD and MAD37

BL21 (DE3) cells carrying the respective clones were used to determine the overexpression of these proteins in *E. coli* cells. FLADAAD and MAD37 are expressed under the control of *tac* promoter present in the expression vector pGEX-6P-2. *tac* promoter is an inducible promoter and expression of the gene under the control of this promoter is induced by the lactose analog isopropyl β-D thiogalactoside (IPTG). All pGEX vectors are also engineered with an internal *lac*Iq gene. The *lac*Iq gene product is a repressor protein that binds to the operator region of the *tac* promoter, preventing expression until induction by IPTG, thus maintaining tight control over expression of the insert. pGEX-6P-2 also have PreScission protease cleavage site which can be used to cleave the fusion protein from the GST-tag.

FLADAAD and MAD37 are expressed as a GST-tagged protein which allows us to purify the proteins by affinity chromatography using glutathione-agarose beads. The molecular weights of the proteins are 82- and 37-kDa respectively, while the size of the GST-tag is 26-kDa, resulting in fusion proteins of molecular weights 108- and 63-kDa respectively. The GST tag can be removed using PreScission protease as this vector contains PreScission protease site between the tag and the cloned gene.

To determine whether these clones overexpress FLADAAD and MAD37, the cells were grown at 37°C till OD_{600nm} reached 0.5. IPTG was added to a final

concentration of 1mM in case of MAD37 and 0.5mM in case of FLADAAD respectively to induce the cells. After induction, the cells were harvested at different time intervals and expression was analysed by SDS-PAGE. Uninduced cells were used as negative control.

Expression of MAD37 was seen in at the induced samples starting from 2 hours post-induction. Fig.11 shows expression of MAD37 at 2, 4 and 6 hours post-induction along with uninduced samples (data not shown for 8 and 16 hours). The levels of expression at different time intervals were found to be similar. The molecular weight of the proteins was confirmed by calculating the Rf (Fig.12). Similarly, expression of FLADAAD was seen in induced sample starting from 2 hour post induction. Fig.13 shows the expresssion of FLADAAD at 0, 2 and 4 hours post induction along with uninduced sample (data not shown for 8 and 16 hours). The levels of expression at different time interval were found to be similar. The molecular weight of the protein was confirmed by calculating the Rf (Fig.14).

Optimization of MAD37 expression

The next step was to optimize the expression level of MAD37 protein. For optimization, we chose to study temperature, IPTG, and time for induction as variables.

Expression studies were preformed at 37 °C, 30°C, and 25°C, using 1mM IPTG for induction. Cells were harvested after 0, 2, and 4 hours of induction and analyzed on a SDS-PAGE (Fig. 11, 15 and 16).

Expression of MAD37 using different concentration (0.1 to 1.5 mM) of IPTG was also done at these different temperatures was also done (data not shown). .However,

expression of MAD37 found to be similar at all concentration of IPTG, so for further studies we selected 0.25mM IPTG concentration.

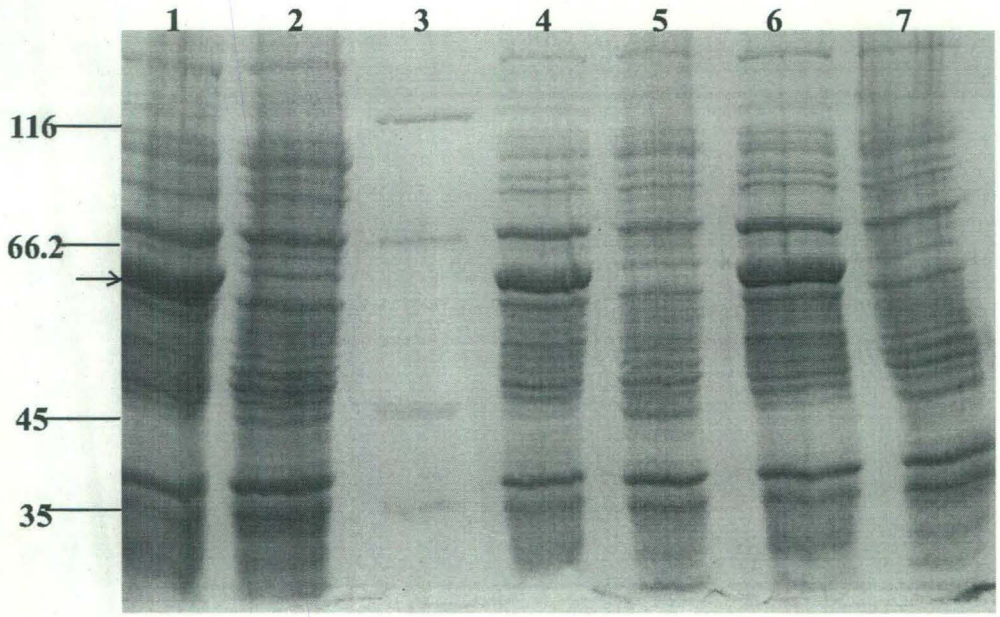

Figure 11: Expression of MAD37 at 37°C induced with 1mM IPTG. Lanes 2, 5, and 7 shows uninduced samples harvested 2, 4 and 6 hours after addition of IPTG in induced samples. Lanes 1, 4, and 6 shows induced sample after 2, 4, and 6 hours of induction. Lane 3 is the molecular weight marker. All molecular sizes in the figure are indicated in kDa.

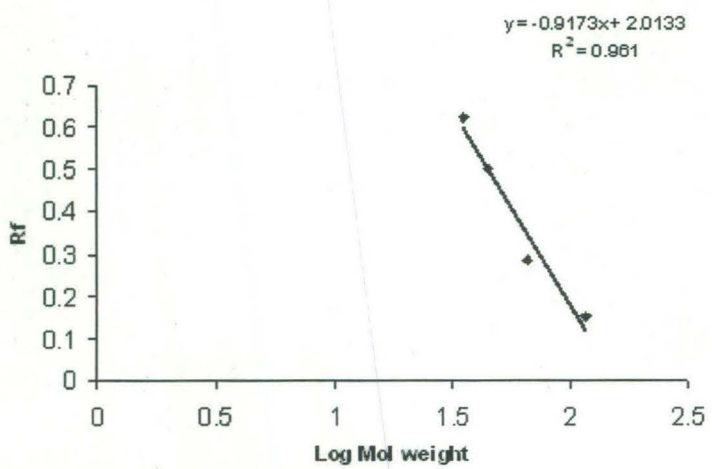

Figure 12: Graph showing molecular weight calculation of MAD37 by plotting Rf v Log Mol weight

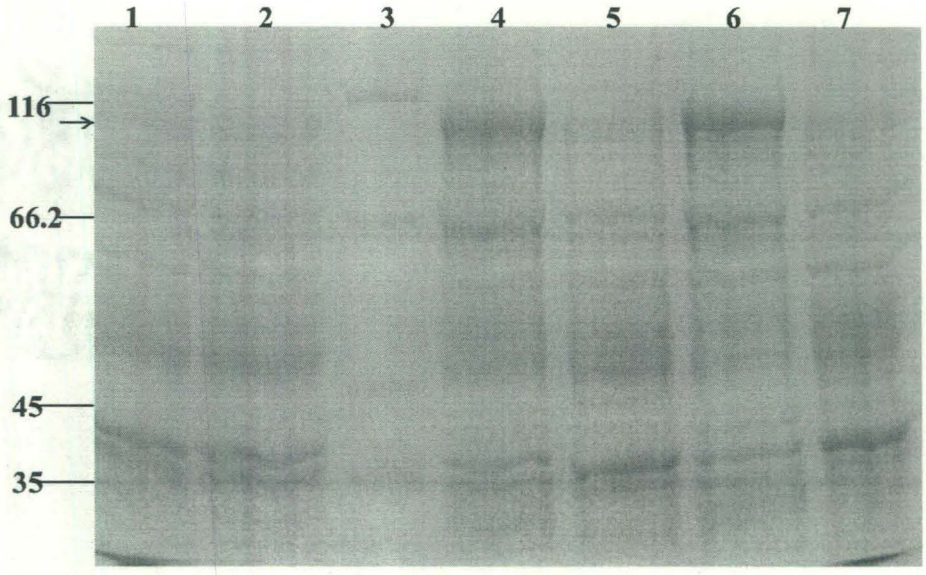

Figure 13: Expression of FLADAAD at 37°C induced with 0.5 mM IPTG. Lanes 1, 4, and 6 shows induced sample after 0, 2, and 4 hours of induction. Lane 2, 5, and 7 are uninduced sample after 0, 2, and 4 hours. Lane 3 is the molecular weight marker. All molecular sizes in the figure are indicated in kDa.

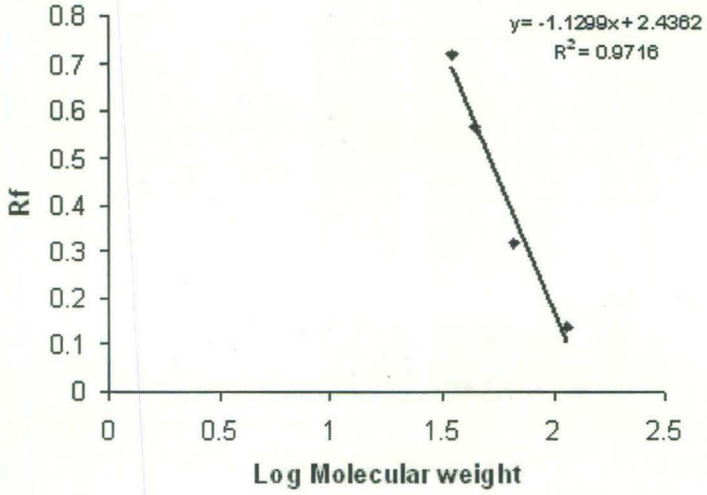

Figure 14: Graph showing molecular weight calculation of FLADAAD by plotting Rf v Log Mol weight

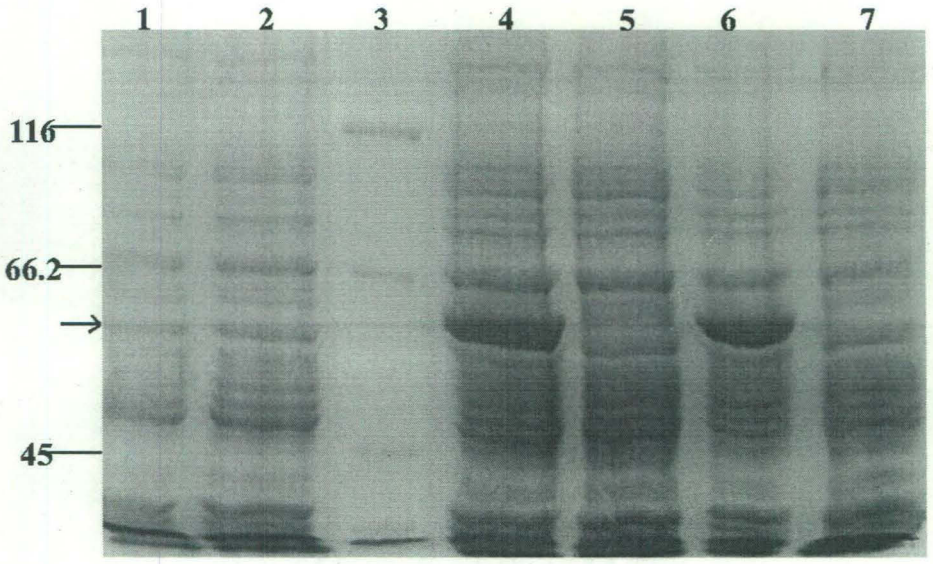

Figure 15: Expression of MAD37 at 30°C induced with 1mM IPTG. Lanes 1, 5, and 7 shows uninduced sample harvested 0, 2, and 4 hours after addition of IPTG in induced samples. Lane 2, 4, and 6 are induced samples after 0, 2 and 4 hours of induction. Lane 3 is the molecular weight marker. All molecular sizes in the figure are indicated in kDa.

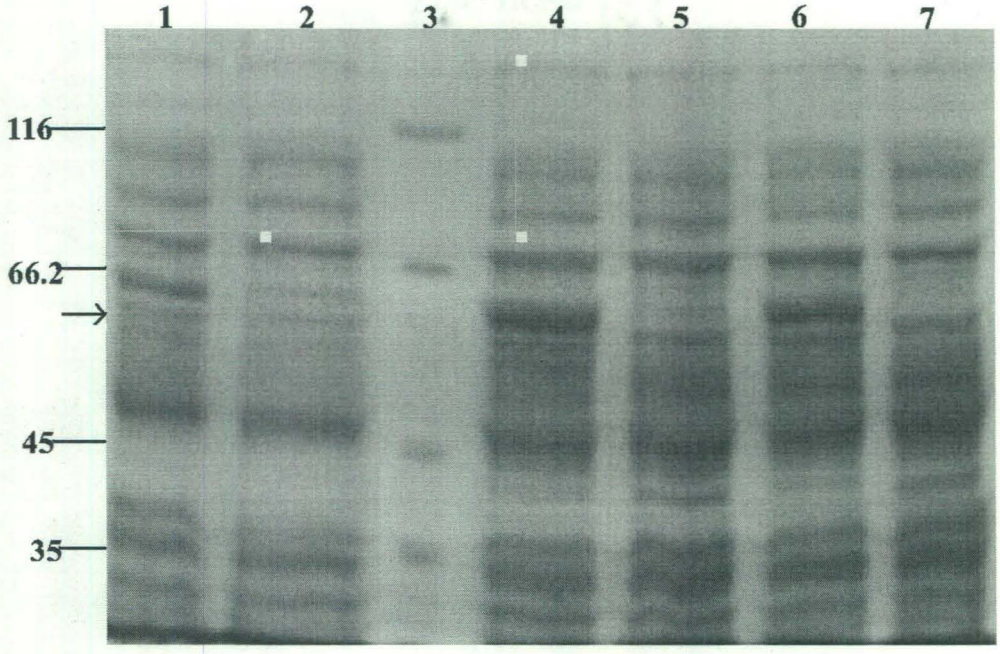

Figure 16: Expression of MAD37 at 25°C induced with 1mM IPTG. Lanes 2, 5, and 7 shows uninduced sample harvested 2, 4 and 6 hours after addition of IPTG in induced samples. Lane 1, 4 and 6 are induced sample after 2, 4, and 6 hours after induction. Lane 3 is the molecular weight marker. All molecular sizes in the figure are indicated in kDa.

Optimization of FLADAAD expression

The same three variables- temperature, IPTG, and time of induction-were selected for optimizing the expression of FLADAAD. Overexpression of ADAAD was seen at 37°C (Fig.13), 30°C, 25°C, and 16°C (data not shown).

Expression of FLADAAD was also carried out using different concentration of IPTG ranging from 0.125 to 1.5 mM (Fig.17). Induction was done at 37°C for 4 hours. The cells were harvested and analysed by SDS-PAGE.

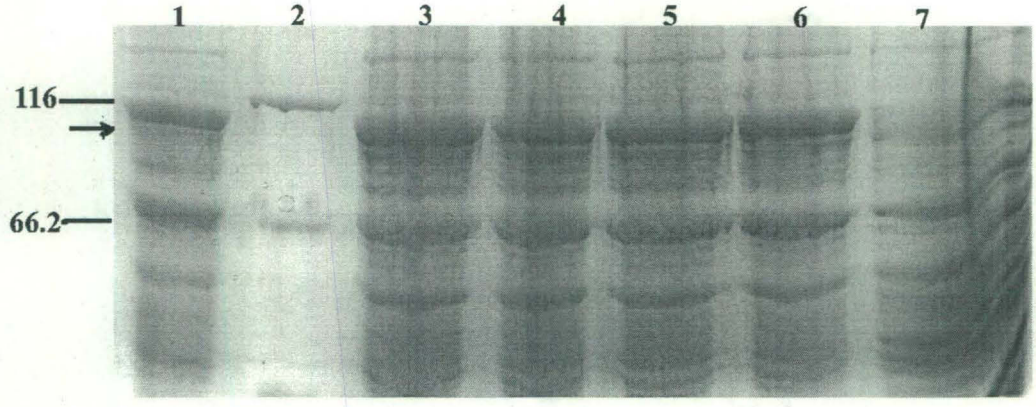

Figure 17: Expression of FLADAAD at 37°C using different concentration of IPTG. Lanes 1, 3, 4, 5, and 6 shows samples induced with 0.125, 0.25, 0.5, 1, and 1.5 mM IPTG. Lane 2 is the molecular weight marker. Lane 7 is the uninduced sample. Samples were incubated for 4 hours after induction with IPTG. All molecular sizes in the figure are indicated in kDa.

Solubilisation of FLADAAD and MAD37

For purification of a protein from a cell, it is necessary that the protein is in the soluble fraction. Most of the time when mammalian proteins are over expressed in *E.coli* cells; a bulk of the protein goes into the insoluble fraction. Conditions like lower growth

temperature and lower IPTG concentration have been known to help in producing proteins that are present in soluble fraction. Different lysis conditions, for example use of β-mercaptoethanol to break disulphide bridges and detergents, have also been known to help in solublisation of overexpressed proteins. So to solublise the overexpressed FLADAAD and MAD37, different conditions were tried out.

During my studies I have found that FLADAAD and MAD37 were not soluble if cells were induced at 37°C or at 30°C even though the expression levels were high (data not shown). Therefore, I experimented with different conditions to solubilise these overexpressed proteins.

Expression of MAD37 at 25°C with 0.25 mM IPTG and presence of 150mM $MgCl_2$, 5mM β-mercaptoethanol and 0.1% (v/v) TritonX-114 in the lysis buffer were found to result in partial solubility of the protein as can be seen from the Fig18 (compare lanes 4 and 5). Therefore, this condition was selected for expression of MAD37 for further studies.

Similarly, for solubilisation of FLADAAD different experiments were performed. FLADAAD was found to be insoluble if induced at 37°C, 30°C, or at 25°C using lysis buffers 6 and 7(Fig 19 and 20). Expression of FLADAAD at 16°C and using lysis buffer 6 was seen to result in partial solubilisation of the protein (Fig.21). Therefore, this condition was selected for purification of the protein.

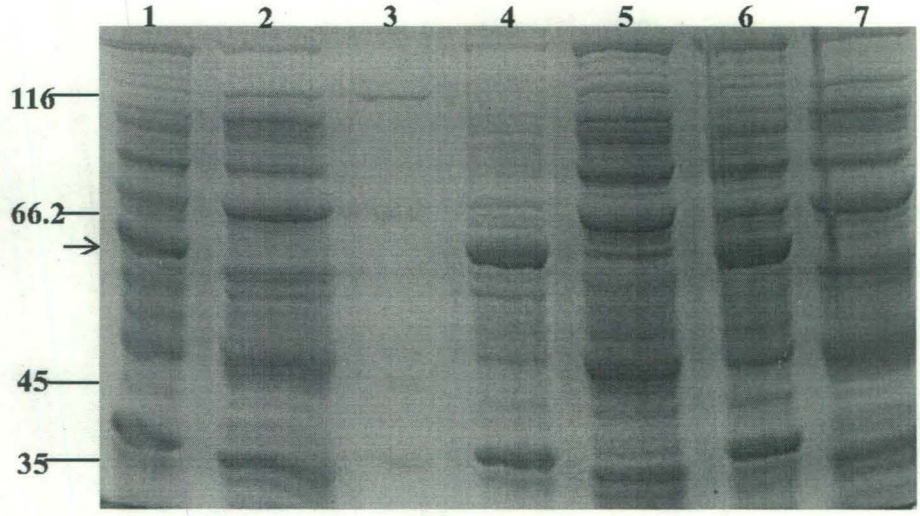

Figure 18: Solubilisation studies of MAD37 at 25°C induced with 0.5mM IPTG. Lanes 1 and 2 are pellet and supernatant of cells incubated in lysis buffer having 5mM β-mercaptoethanol and 150mM $MgCl_2$. Lanes 4 and 5 are pellet and supernatant of cell lysed in lysis buffer 3 with (0.1% v/v) Triton –X114(appendix). Lanes 6 and 7 is pellet and supernatant of cells induced with 0.25mM IPTG, incubated in lysis buffer 1 (appendix). Lane 3 is the molecular weight marker. All molecular sizes in the figure are indicated in kDa.

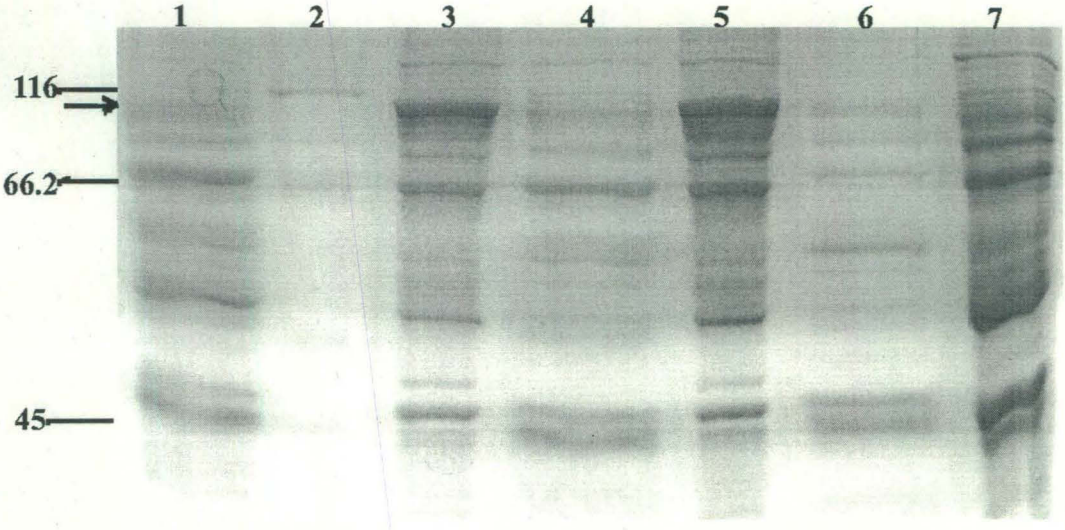

Figure 19: Solubilisation studies of FLADAAD at 30°C using 0.25 mM IPTG under different lysis buffer conditions. Lanes 1 and 3 are supernatant and pellet fraction of 2 hours induced sample in which the cells were incubated in lysis buffer 7. Lanes 4 and 5 were supernatant and pellet fraction of 2 hours induced sample in which the cells are incubated in lysis buffer 6. Lanes 6 and 7 were supernatant and pellet fraction of uninduced sample. Lane 2 is the molecular weight protein in kDa

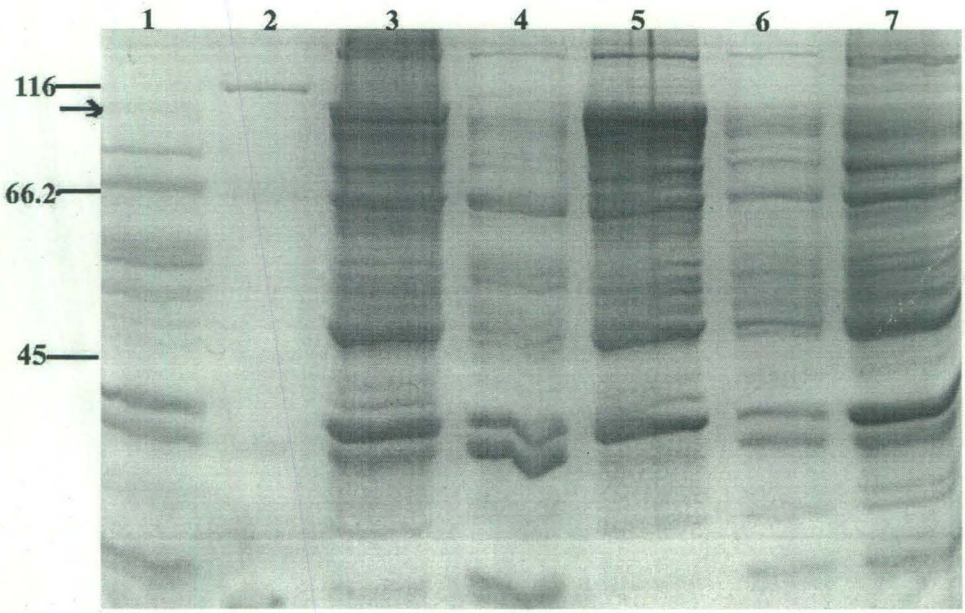

Figure 20: Solubilisation studies of FLADAAD at 25°C using 0.25 mM IPTG under different lysis buffer condition. Lane 1 and 3 are supernatant and pellet fraction of 2 hours induced sample in which the cells were incubated in lysis buffer 5. Lanes 4 and 5 are supernatant and pellet fraction of 2 hours induced sample in which the cells were incubated in lysis buffer 7. Lanes 6 and 7 are supernatant and pellet fraction of uninduced sample. Lane 2 is the molecular weight protein in kDa

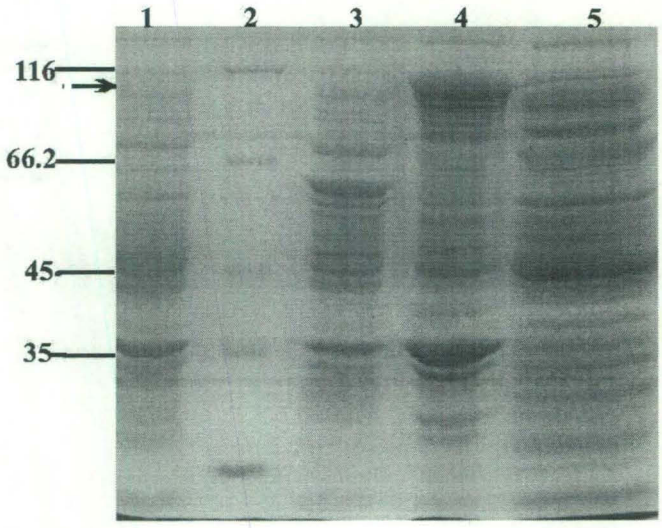

Figure 21: Solubilisation studies of FLADAAD at 16°C using 0.25 mM IPTG under different lysis buffer conditions. Lanes 1 and 3 are supernatant and pellet fraction of 2 hours induced sample in which the cells were incubated in lysis buffer 7. Lanes 4 and 5 are supernatant and pellet fraction of 2 hours induced sample in which the cells were incubated in lysis buffer 6. Lanes 6 and 7 are pellet and supernatant fraction of uninduced sample. Lane 2 is the molecular weight marker. All molecular sizes in the figure are indicated in kDa.

Purification of FLADAAD and MAD37

FLADAAD and MAD37 were purified as GST-tagged protein as described in *Materials and Methods.*

Purification of FLADAAD from 1L LB media was done by harvesting the cells after induction at 16°C with 0.25mM IPTG. The supernatant after lysis and clarification by centrifugation was loaded onto GST-agarose column. The bound protein was eluted with glutathione and the fractions were analyzed by SDS-PAGE. Protein was estimated by Bradford method and the method gave us a yield of 1.5mg/L protein (Fig.22). However, subsequent purification gave a very low yield around 0.3-0.5 mg/L. The conditions for purification, therefore, need to be further optimized.

Purification of MAD37 from 1L culture was done using the same method as for FLADAAD. The purification procedure resulted in a yield of 0.4mg/L of protein (Fig.25)

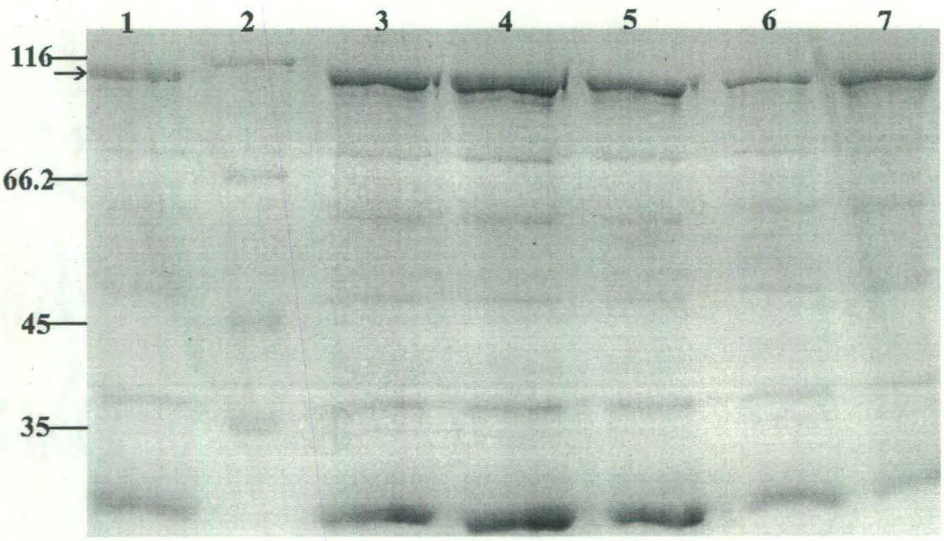

Figure 22: Purification of FLADAAD. Lane 1,3,4,5,6 and 7 are elution fraction of 2^{nd} ,3^{rd} ,4^{th} 6^{th} ,8^{th} and 10^{th} eluate. Lane 2 is the molecular weight marker in kDa.

Removal of GST tag

The next step after purification was to remove the GST-tag so as to release the native protein, which could be used for further biophysical analysis. The GST-tag was released from the protein by digestion of the protein with PreScission protease (Fig.23). PreScission protease was purchased from Amersham Biosciences. The protease has a GST-tag which enables it to be purified from the protein of interest after cleavage of the GST-tag by using the glutathione agarose beads. The purified protein was dialyzed overnight against PreScission protease buffer PreScission protease was added to the protein sample and incubated at 10°C for 12 hours.

GST-tag and Prescission protease were subsequently separated from FLADAAD by mixing the digestion mix with gluatathione-agarose beads pre-equilibrated with cleavage buffer. The mixture was then centrifuged at 2500 rpm for 5 minutes. The supernatant was carefully removed by pipetting into a fresh tube. The protein was then analysed by SDS PAGE and protein estimation was done using Bradford reagent (Fig .24). This protein was used for further biochemical and structural analysis.

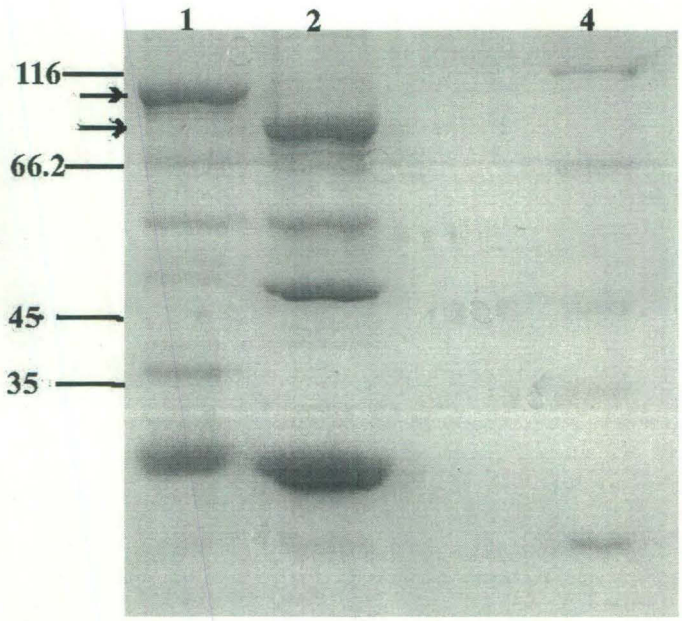

Figure 23: Cleavage of GST-tag from FLADAAD by Precision protease. Lane 1 shows the GST-tagged protein. Lane 2 shows the FLADAAD with out GST-tag. Lane 3 is the molecular weight marker. All molecular sizes in this figure are in kDa.

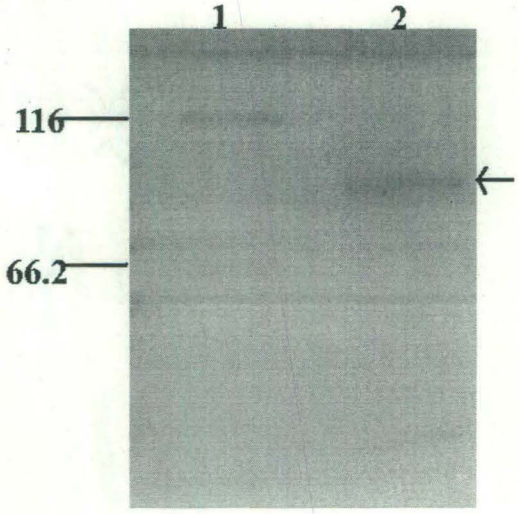

Figure 24: Purification of FLADAAD from GST after cleavage with PreScission protease. Lane 1 is marker in kDa .Lane 2 show the purified FLADAAD with out no GST (indicated by the arrow)

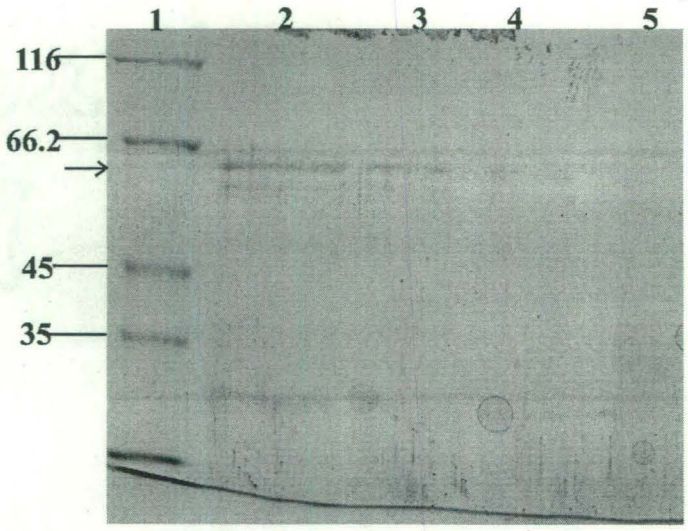

Figure 25: Purification of MAD37. Lane 2, 3, 4 and 5 are elution fraction of 4^{th} 6^{th}, 8th and 10^{th} eluate. Lane 1 is the marker

ATPase Assay

FLADAAD is a DNA dependent ATPase enzyme. ATPase assay were carried out to check the activity of the protein. In this study the Pi release by due to ATP hydrolysis was detected using the method described in King(32).

ATPase assay was carried out in presence and absence of stem loop DNA. ATPase assay with FLADAAD show very little DNA dependent activity. The specific activity of the protein was found to be 10 nmoles Pi release/mg/min

Fluorescence Studies

Fluorescence studies were carried out to calculate the K_d for ATP and DNA binding. In this study, fluorescence intensity of tryptophan residues was monitored to see if there was any change in fluorescence intensity when titration was initiated by addition of ATP and DNA. Calculation for K_d was done as explained in *Material and Methods*

Fluorescence studies were carried out for both MAD37 and FLADAAD to calculate the binding constant for ATP and DNA. Experiments were carried out as mention in *Materials and Methods.*

Binding studies with MAD37 shows that ATP binding is 4.27 ± 0.4715 mM (Fig.26). Experiment was also carried out to calculate the K_d for DNA binding with MAD37 but the Kd can not be calculated because the reaction has not reached saturation (Fig.28and Fig.29). The K_d for DNA binding in absence of ATP was calculated to be 3.32 ± 0.71 nM (Fig.30 and Fig.31). Binding studies carried out with FLADAAD shows that K_d for ATP binding in absence of any added DNA effector was calculated to be 2.22 ±.0.59mM (Fig.32 and Fig.33)

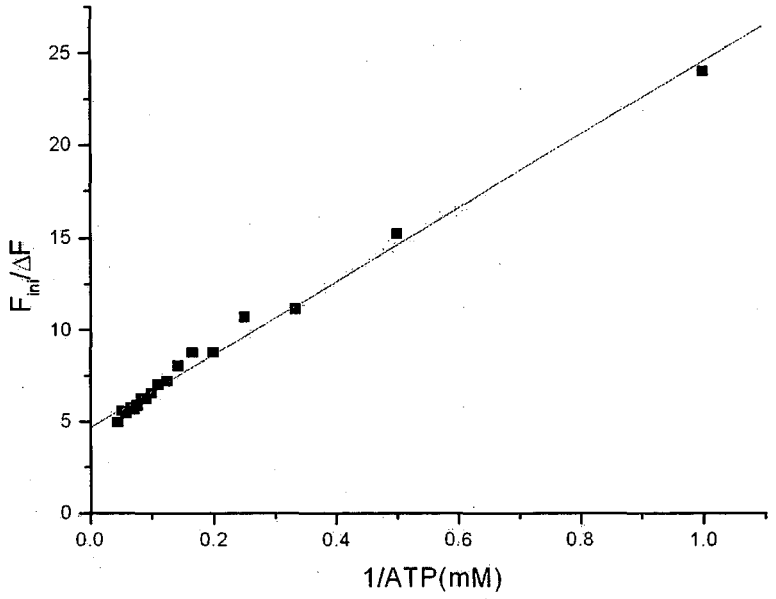

Figure 26: Double reciprocal plot of the change in Fluorescence against ligand concentration (ATP) for MAD37. ΔF is the change in fluorescence.

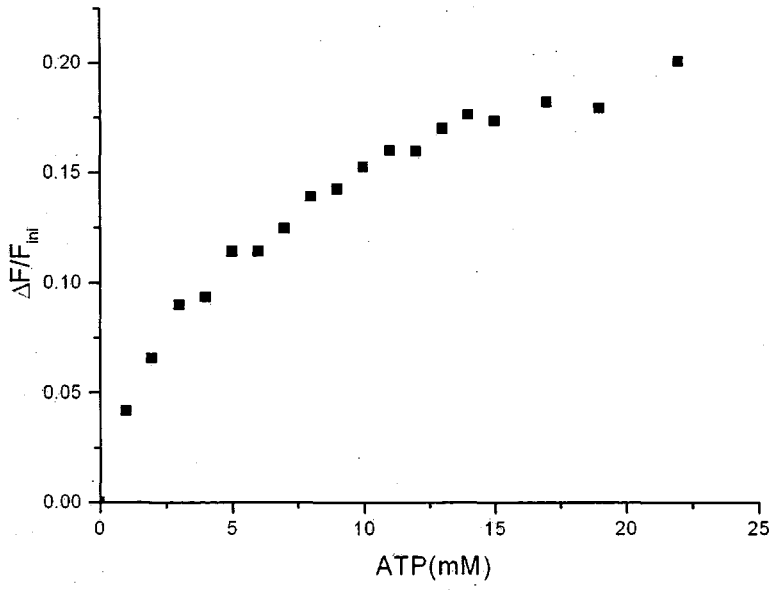

Figure 27: Graph showing the change in Fluorescence intensity with increase concentration of ATP for MAD37

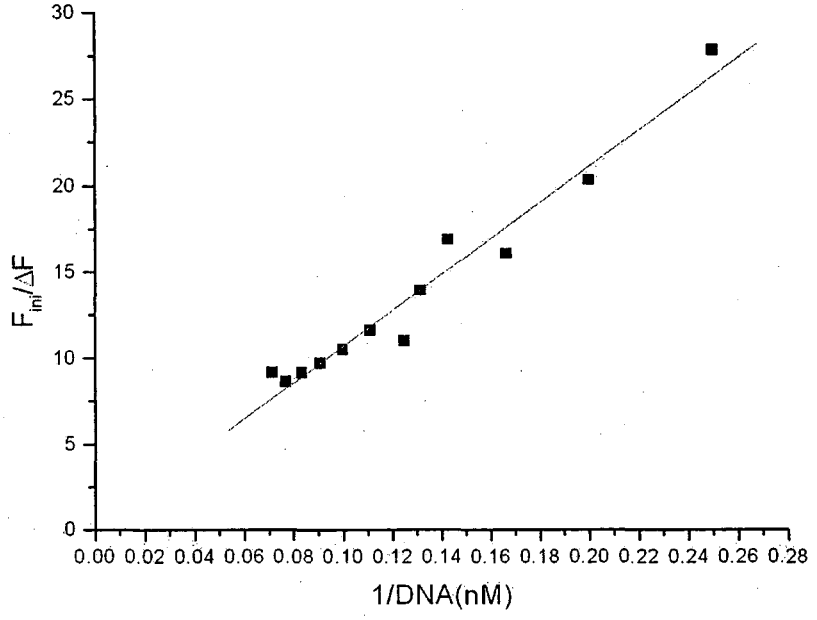

Figure 28: Double reciprocal plot of the change in Fluorescence against ligand concentration (DNA) for MAD37.ΔF is change in fluorescence.

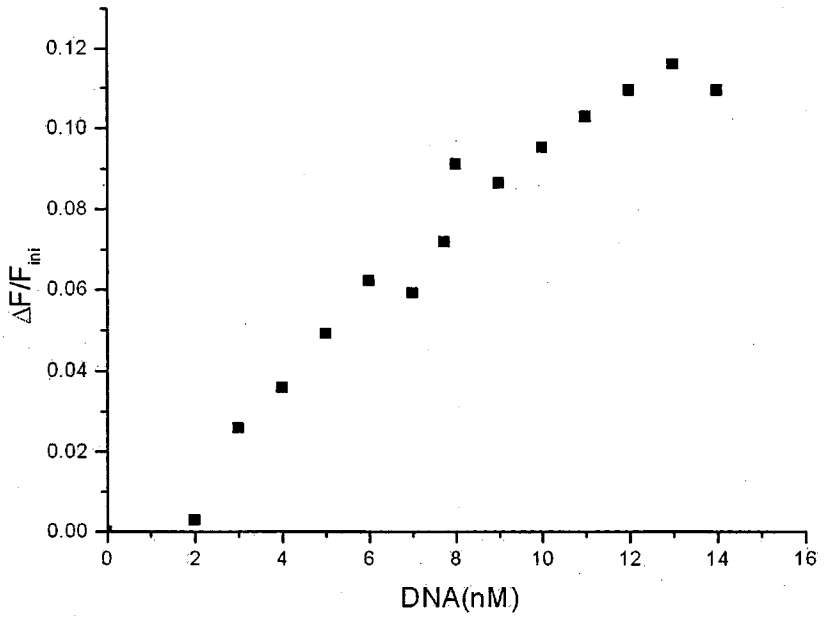

Figure 29: Graph showing the change in Fluorescence intensity with increase concentration of DNA for MAD37. ΔF is change in fluorescence

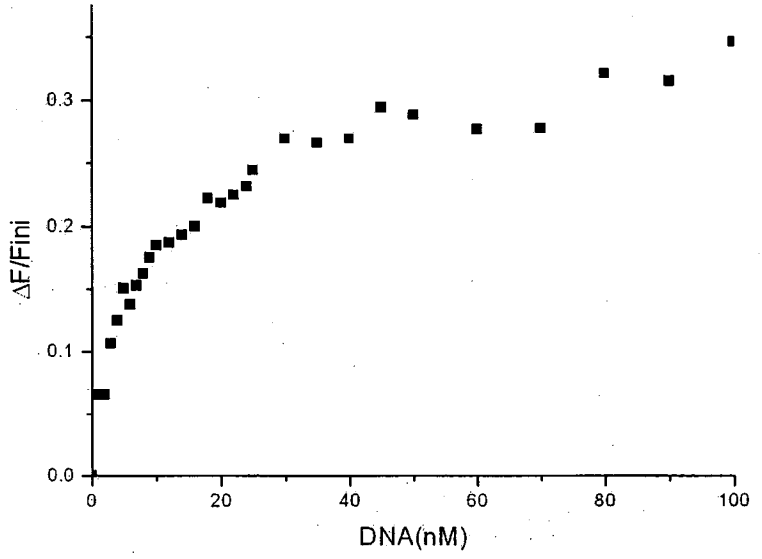

Figure 30: Graph showing the change in Fluorescence intensity with increase concentration of DNA for FLADAAD.

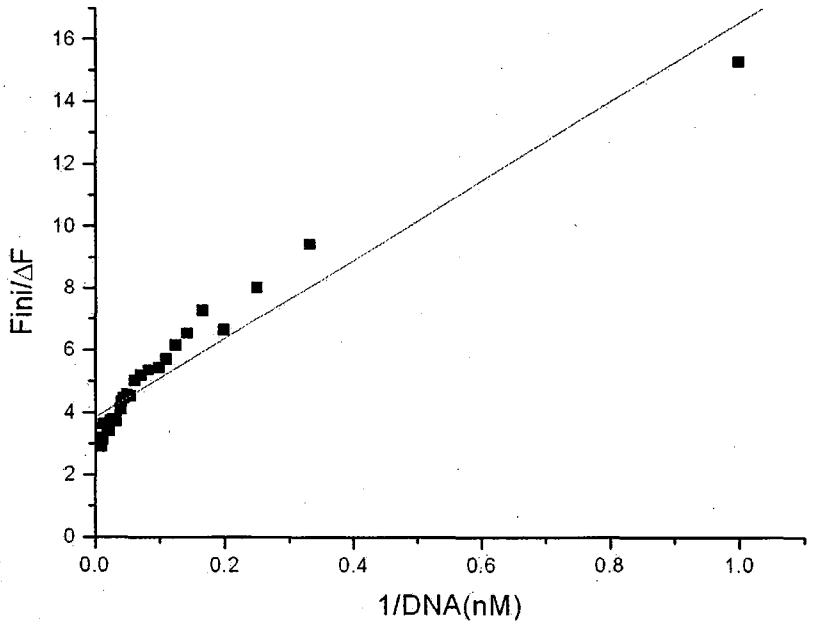

Figure 31: Double reciprocal plot of the change in Fluorescence against ligand concentration (DNA) of FLADAAD

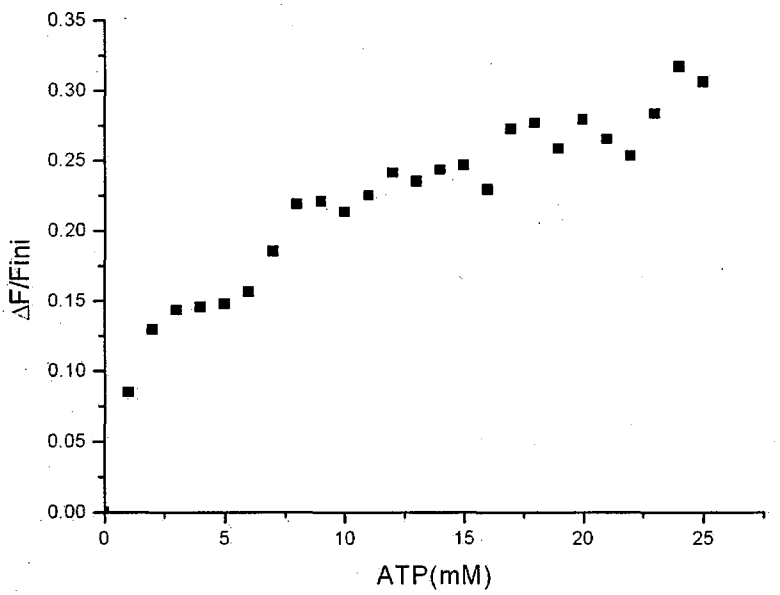

Figure 32: Graph showing the change in Fluorescence intensity with increase concentration of ATP for FLADAAD

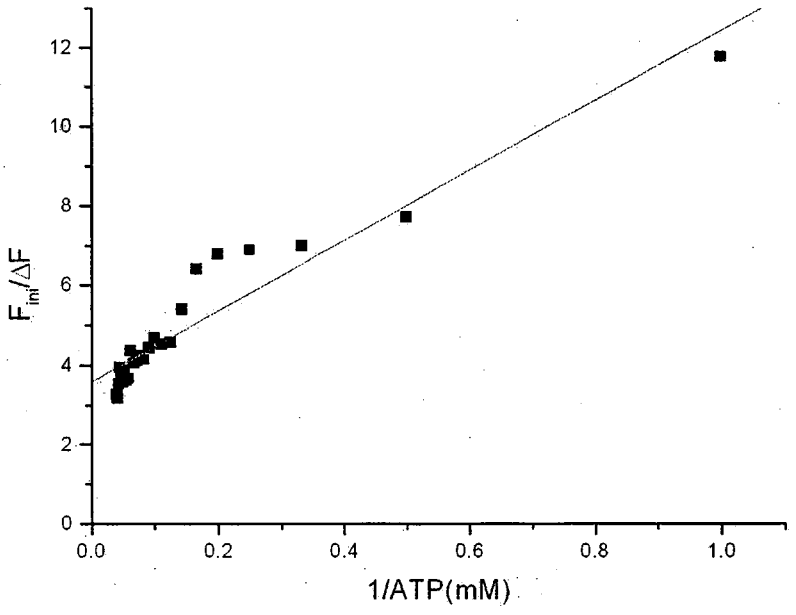

Figure 33: Double reciprocal plot of the change in Fluorescence against ligand concentration (ATP) for FLADAAD.

DISCUSSION

ADAAD is a member of the SWI/SNF family of proteins(21). This protein, known as DNA-dependent ATPase A, was first purified from calf thymus(42). The parent protein of ADAAD is 105-kDa, which undergoes proteolytic cleavage to yield two polypeptides of 68- and 82-kDa. The 82-kDa protein is known as Active DNA-dependent ATPase A (ADAAD) as it retains all the seven helicase motifs and is capable of hydrolyzing ATP in the presence of DNA effector. ADAAD, however, lacks the N-terminal region.

ADAAD is capable of DNA-dependent ATPase activity. The protein recognizes DNA molecules that possess a double-strand to single-strand transition regions. Thus, DNA molecules containing stem-loop structures or bulges or mismatches were found to be the most effective effectors of ATPase activity. The human homolog of DNA-dependent ATPase A is SMARCAL1, which is known to cause Schmike Immuno-Osseous Dysplasia, a rare autosomal recessive disorder(6).

The SWI/SNF family of proteins belongs to the SF2 superfamily of helicases. One of the most important characteristics of SF2 is the presence of the conserved DExx box; incase of ADAAD the motif is a DESH box.

In this study ADAAD was amplified from pCP101. The template pCP101 is a His-tag vector carrying the ADAAD gene. ADAAD was amplified from this vector using specific primers and then cloned into pGEX-6P-2 which is a GST-tag vector. Expression of ADAAD in pGEX-6P-2 will help in purifying the protein by affinity chromatography using glutathione-agarose beads. Moreover, the tag can be cleaved using PreScission protease), which otherwise is not possible in His-tag protein. This is important especially

when trying to perform structural studies as the tag might block the active site or alter the conformation of the protein.

For this study I have also cloned the deletion mutant of ADAAD called MAD37. The gene for this protein was amplified from pRM102 plasmid. This plasmid carries a stop codon at position 333, which leads to expression of truncated protein of 37-kDa. Sequence analysis and *in silico* translation show that the codon for lysine has been mutated into a stop codon. MAD37 possesses only three helicase motifs; the GKT box (Walker A motif), the Ia motif and the DESH box (Walker B).

Expression studies show that both FLADAAD and MAD37 are overexpressed in BL21 (DE3) *E.coli* cells. Both the proteins express at different temperatures (37°C, 30°C, 25°C, and 16°C) and IPTG concentrations. As pGEX expression vectors use *tac* promoters, the proteins can also be expressed in DH5α cells. MAD37 was found to be expressing in DH5α cells at 37°C using 1mM IPTG (data not shown).

Solubilisation studies have shown that induction at 37°C and 30°C does not result in solubilisation of the proteins even though expression is high. Expression of protein at lower temperature i.e. 25°C and 16°C helps in solubilising the protein. Growing cell at 25°C and 16°C leads to the slow growth of the cells and hence expression of foreign protein is slow which helps in proper folding of protein so that most of it is in soluble form. Whereas at 37°C and 30°C cell growth is rapid, so is the expression of the proteins leading to bulk of the protein forming inclusion bodies which are insoluble.

Salt and β-mercaptoethanol are also important for solubilising the protein. Lysis buffer having 10mM β–mercaptoethanol and 150mM $MgCl_2$ was found to improve solubilisation of the protein. This could be due to the fact that motif II in ADAAD is

involved in Mg^{+2} binding, so we hypothesized that the presence of $MgCl_2$ in lysis buffer might help in proper folding of the protein(13). β–mercaptoethanol provides the protein with the reducing environment, so that when the protein comes out from the cell in contact with the buffer, it is not denatured or misfolded. We found that TritonX-114 also helped in solubilising the proteins as it is known that hydrophobic tail of the detergent bind to hydrophobic region of the protein and hydrophilic part of the detergent interact with water, therefore keeping the protein solution.

MAD37 and FLADAAD were purified by affinity chromatography using glutathione-agarose beads. Protein was eluted using buffer having 10mM reduced glutathione. Initial studies show that most of the protein remains bound to the beads even after adding elution buffer. The elution conditions were improved by addition of 100mM NaCl in the elution buffer which resulted in better elution of the bound protein. The first batch of purification of FLADAAD gave a yield of 1.5mg/L, but in subsequent batch of purification a very low yield of 0.3-0.4mg/L was obtained. During the first batch of purification of the protein, the elution buffer did not have β–mercaptoethanol and glycerol. This might have been the reason for the low yield of the protein in subsequent batch, but this has to be ascertained. Regenerated beads were also used in later purification, which could be another reason for the low yield of the protein. The yield of MAD37 is 0.4 mg/L which is quite low, so further optimization of purification procedure is needed. The GST tag from FLADAAD was removed by PreScission protease.

Cleavage of the tag was done in solution. The eluted protein was dialysed against cleavage buffer to exchange out the elution buffer, concentrated using concentrators, and treated with PreScission Protease. Cleavage of the tag while the protein was bound to the

column was also tried, but the cleavage of the protein was found to be very inefficient. GST tag and PreScission protease were separated from FLADAAD by mixing the digestion mix with glutathione-agarose beads. The GST-tag and PreScission Protease which is also a GST tagged protein bound to the beads leaving the tagless FLADAAD in the supernatant, which came out in the flowthrough.

ATPase activity for ADAAD was also carried out in presence of stem-loop DNA. ATP hydrolysis was seen both in the presence and absence on DNA, even though there is slight increase in presence of DNA. DNA-dependent activity was not seen because of the contamination of DNA from purification (personal communication from Dr. Joel W. Hockensmith), so removal of the DNA is required to observe the DNA-dependent activity of FLADAAD. This can be done by passing the protein through DEAE-column in presence of 50mM K_2SO_4 to remove the DNA. It can also be done by ultracentrifugation after addition of 2M NaCl to disrupt protein-DNA interaction. The procedure needs to be optimized.

The specific activity of FLADAAD is 10 nmole Pi release/mg/min which is quite low compare to previous studies which shows that ADAAD have specific activity 16 μmole Pi release/mg/min(44).

Fluorescence studies to study ATP and DNA binding were done using both MAD37 and FLADAAD. In my studies, fluorescence intensity of tryptophan residues was monitored by exciting the protein at 295nm. The emission was monitored from 310-400 nm. Change in fluorescence intensity was monitored with increased in ligand concentration. In case of FLADAAD the K_d for DNA was found to be 3.32 nM which usual for SWI/SNF motor domain(47, 60). ATP hydrolysis assay which were carried out

previously for ADAAD with stem loop DNA show that K_d for DNA is 1.9 ± 0.4nM(44). K_d for DNA binding by MAD37 was calculated to be 520 ±1.28 nM. We can see that K_d for ADAAD from fluorescence is comparable with the K_d calculated by ATP hydrolysis. K_d for DNA binding of MAD37 was found to be 270-fold higher than the K_d for DNA of FLADAAD. From this study we can see that FLADAAD binding to the DNA is strong whereas MAD37 binding to the DNA is very weak. This shows that other motifs (III, IV V and VI) which are not present in MAD37 are responsible for DNA binding. ATP binding was also calculated by fluorescence studies and it was found to be 2.22 ± 0.59 mM which is comparable to the K_d calculated by ATP hydrolysis (2.76 mM)(43). K_d for ATP binding for MAD37 was also calculated by fluorescence and it was found to be 4.27± 0.71mM.

The binding of MAD37 to ATP is comparable to FLADAAD as both the proteins have the GKT box which is known to be necessary for ATP binding(61). This shows that motif I, Ia and II are involved in ATP binding. Binding of FLADAAD to DNA is 270-fold higher as compared to the MAD37. MAD37 does not have the other helicase motif i.e. motif III, IV, V and VI as compares to FLADAAD which have the entire seven motif. This shows that the other motifs, which are missing from MAD37, are involved in DNA binding

According to crystal structure of Rad54 and SSoRad54 there are two sub-domains of the motor domain termed domain 1 and domain 2(18). The domain1 contains the motifs I, Ia, II and III while the domain 2 possesses the motifs IV, V and VI. MAD37 is most similar to domain 1 since it has GKT box (motif I), Ia and DESH box (Motif II) and DNA binding is almost same as domain 1 of SsRad54 (0.22+-0.1 μM).

DNA binding of FLADAAD is 3.32 nM, which is 30-folds lower as compared to SsoRad54 (0.1+-0.02 μM). This could be that using stem loop DNA can result in increase in DNA binding as it has been shown before that it is a good effector for ADAAD whereas in SsoRad54 they have use dsDNA only(44). The effector studies have not been done with other SWI/SNF proteins; therefore, it is very difficult to comment on the very high K_d shown by Rad54.

K_d for ATP binding are almost the same (within experimental error) for FLADAAD and MAD37 which suggests that domain 1 of ADAAD is necessary and probably sufficient for ATP binding. So far studies for ATP binding for FLADAAD and other SWI/SNF motor domains have not been done except for Hockensmith *et al.* who calculated the K_d for ATP for the native protein to be 0.76mM(28).

Further studies need to be done to show domain 2 alone can binds to DNA even though SsoRad54 domain 2 have be reported that it does have any DNA binding(18).

Studies also need to be done to show whether ATP and DNA binding are interdependent and which residues are involved in DNA and ATP binding. It will also be very interesting to see whether mutation or modification of the tryptophan residue would have any effect on the ATPase activity and binding of ATP and DNA. Furthermore mechanism of how DNA and ATP binding are coordinated to help in ATP hydrolysis needs to be elucidated.

REFERENCES

1. **ALLFREY, V. G., R. FAULKNER, and A. E. MIRSKY.** 1964. ACETYLATION AND METHYLATION OF HISTONES AND THEIR POSSIBLE ROLE IN THE REGULATION OF RNA SYNTHESIS. Proc.Natl.Acad.Sci.U.S.A **51**:786-794.

2. **Arents, G., R. W. Burlingame, B. C. Wang, W. E. Love, and E. N. Moudrianakis.** 1991. The nucleosomal core histone octamer at 3.1 A resolution: a tripartite protein assembly and a left-handed superhelix. Proc.Natl.Acad.Sci.U.S.A **88**:10148-10152.

3. **Arents, G. and E. N. Moudrianakis.** 1993. Topography of the histone octamer surface: repeating structural motifs utilized in the docking of nucleosomal DNA. Proc.Natl.Acad.Sci.U.S.A **90**:10489-10493.

4. **Bazett-Jones, D. P., J. Cote, C. C. Landel, C. L. Peterson, and J. L. Workman.** 1999. The SWI/SNF complex creates loop domains in DNA and polynucleosome arrays and can disrupt DNA-histone contacts within these domains. Mol.Cell Biol. **19**:1470-1478.

5. **Becker, P. B. and W. Horz.** 2002. ATP-dependent nucleosome remodeling. Annu.Rev.Biochem. **71**:247-273.

6. **Boerkoel, C. F., H. Takashima, J. John, J. Yan, P. Stankiewicz, L. Rosenbarker, J. L. Andre, R. Bogdanovic, A. Burguet, S. Cockfield, I. Cordeiro, S. Frund, F. Illies, M. Joseph, I. Kaitila, G. Lama, C. Loirat, D. R. McLeod, D. V. Milford, E. M. Petty, F. Rodrigo, J. M. Saraiva, B. Schmidt, G. C. Smith, J. Spranger, A. Stein, H. Thiele, J. Tizard, R. Weksberg, J. R. Lupski, and D. W. Stockton.** 2002. Mutant chromatin remodeling protein SMARCAL1 causes Schimke immuno-osseous dysplasia. Nat.Genet. **30**:215-220.

7. **Bokenkamp, A., M. deJong, J. A. van Wijk, D. Block, J. M. van Hagen, and M. Ludwig.** 2005. R561C missense mutation in the SMARCAL1 gene associated with mild Schimke immuno-osseous dysplasia. Pediatr.Nephrol. **20**:1724-1728.

8. **Bradford, M. M.** 1976. A rapid and sensitive method for the quantitation of microgram quantities of protein utilizing the principle of protein-dye binding. Anal.Biochem. **72**:248-254.

9. **Brzeski, J. and A. Jerzmanowski.** 2003. Deficient in DNA methylation 1 (DDM1) defines a novel family of chromatin-remodeling factors. J.Biol.Chem. **278**:823-828.

10. **Cairns, B. R., Y. J. Kim, M. H. Sayre, B. C. Laurent, and R. D. Kornberg.** 1994. A multisubunit complex containing the SWI1/ADR6, SWI2/SNF2, SWI3,

SNF5, and SNF6 gene products isolated from yeast. Proc.Natl.Acad.Sci.U.S.A **91**:1950-1954.

11. **Carlson, M. and B. C. Laurent**. 1994. The SNF/SWI family of global transcriptional activators. Curr.Opin.Cell Biol. **6**:396-402.

12. **Carlson, M., B. C. Osmond, and D. Botstein**. 1981. Mutants of yeast defective in sucrose utilization. Genetics **98**:25-40.

13. **Caruthers, J. M. and D. B. McKay**. 2002. Helicase structure and mechanism. Curr.Opin.Struct.Biol. **12**:123-133.

14. **Cherry, S. R. and D. Baltimore**. 1999. Chromatin remodeling directly activates V(D)J recombination. Proc.Natl.Acad.Sci.U.S.A **96**:10788-10793.

15. **Cote, J., C. L. Peterson, and J. L. Workman**. 1998. Perturbation of nucleosome core structure by the SWI/SNF complex persists after its detachment, enhancing subsequent transcription factor binding. Proc.Natl.Acad.Sci.U.S.A **95**:4947-4952.

16. **Cote, J., J. Quinn, J. L. Workman, and C. L. Peterson**. 1994. Stimulation of GAL4 derivative binding to nucleosomal DNA by the yeast SWI/SNF complex. Science **265**:53-60.

17. **Delmas, V., D. G. Stokes, and R. P. Perry**. 1993. A mammalian DNA-binding protein that contains a chromodomain and an SNF2/SWI2-like helicase domain. Proc.Natl.Acad.Sci.U.S.A **90**:2414-2418.

18. **Durr, H., C. Korner, M. Muller, V. Hickmann, and K. P. Hopfner**. 2005. X-ray structures of the Sulfolobus solfataricus SWI2/SNF2 ATPase core and its complex with DNA. Cell **121**:363-373.

19. **Eisen, J. A., K. S. Sweder, and P. C. Hanawalt**. 1995. Evolution of the SNF2 family of proteins: subfamilies with distinct sequences and functions. Nucleic Acids Res. **23**:2715-2723.

20. **Fan, H. Y., X. He, R. E. Kingston, and G. J. Narlikar**. 2003. Distinct strategies to make nucleosomal DNA accessible. Mol.Cell **11**:1311-1322.

21. **Flaus, A., D. M. Martin, G. J. Barton, and T. Owen-Hughes**. 2006. Identification of multiple distinct Snf2 subfamilies with conserved structural motifs. Nucleic Acids Res. **34**:2887-2905.

22. **Flaus, A. and T. Owen-Hughes**. 2004. Mechanisms for ATP-dependent chromatin remodelling: farewell to the tuna-can octamer? Curr.Opin.Genet.Dev. **14**:165-173.

23. **Gawronski, J. D. and D. R. Benson**. 2004. Microtiter assay for glutamine synthetase biosynthetic activity using inorganic phosphate detection. Anal.Biochem. **327**:114-118.

24. **Geng, F., Y. Cao, and B. C. Laurent**. 2001. Essential roles of Snf5p in Snf-Swi chromatin remodeling in vivo. Mol.Cell Biol. **21**:4311-4320.

25. **Gorbalenya, A. E., E. V. Koonin, A. P. Donchenko, and V. M. Blinov**. 1988. A novel superfamily of nucleoside triphosphate-binding motif containing proteins which are probably involved in duplex unwinding in DNA and RNA replication and recombination. FEBS Lett. **235**:16-24.

26. **Guyon, J. R., G. J. Narlikar, S. Sif, and R. E. Kingston**. 1999. Stable remodeling of tailless nucleosomes by the human SWI-SNF complex. Mol.Cell Biol. **19**:2088-2097.

27. **Hassan, A. H., P. Prochasson, K. E. Neely, S. C. Galasinski, M. Chandy, M. J. Carrozza, and J. L. Workman**. 2002. Function and selectivity of bromodomains in anchoring chromatin-modifying complexes to promoter nucleosomes. Cell **111**:369-379.

28. **Hockensmith, J. W., A. F. Wahl, S. Kowalski, and R. A. Bambara**. 1986. Purification of a calf thymus DNA-dependent adenosinetriphosphatase that prefers a primer-template junction effector. Biochemistry **25**:7812-7821.

29. **Imbalzano, A. N., G. R. Schnitzler, and R. E. Kingston**. 1996. Nucleosome disruption by human SWI/SNF is maintained in the absence of continued ATP hydrolysis. J.Biol.Chem. **271**:20726-20733.

30. **Jones, K. A. and J. T. Kadonaga**. 2000. Exploring the transcription-chromatin interface. Genes Dev. **14**:1992-1996.

31. **Kassabov, S. R., B. Zhang, J. Persinger, and B. Bartholomew**. 2003. SWI/SNF unwraps, slides, and rewraps the nucleosome. Mol.Cell **11**:391-403.

32. **King, E. J., M. A. Abul-Fadl, and P. G. Walker**. 1951. King-Armstrong Phosphatase Estimation by the Determination of Liberated Phosphate. J.Clin.Pathol. **4**:85-91.

33. **Kornberg, R. D.** 1974. Chromatin structure: a repeating unit of histones and DNA. Science **184**:868-871.

34. **Kwon, H., A. N. Imbalzano, P. A. Khavari, R. E. Kingston, and M. R. Green**. 1994. Nucleosome disruption and enhancement of activator binding by a human SW1/SNF complex. Nature **370**:477-481.

35. **Lachner, M., D. O'Carroll, S. Rea, K. Mechtler, and T. Jenuwein**. 2001. Methylation of histone H3 lysine 9 creates a binding site for HP1 proteins. Nature **410**:116-120.

36. **Langst, G. and P. B. Becker**. 2001. Nucleosome mobilization and positioning by ISWI-containing chromatin-remodeling factors. J.Cell Sci. **114**:2561-2568.

37. **Laurent, B. C., I. Treich, and M. Carlson**. 1993. The yeast SNF2/SWI2 protein has DNA-stimulated ATPase activity required for transcriptional activation. Genes Dev. 7:583-591.

38. **Linder, P., P. F. Lasko, M. Ashburner, P. Leroy, P. J. Nielsen, K. Nishi, J. Schnier, and P. P. Slonimski**. 1989. Birth of the D-E-A-D box. Nature **337**:121-122.

39. **Lorch, Y., M. Zhang, and R. D. Kornberg**. 1999. Histone octamer transfer by a chromatin-remodeling complex. Cell **96**:389-392.

40. **Luger, K., A. W. Mader, R. K. Richmond, D. F. Sargent, and T. J. Richmond**. 1997. Crystal structure of the nucleosome core particle at 2.8 A resolution. Nature **389**:251-260.

41. **Lusser, A. and J. T. Kadonaga**. 2003. Chromatin remodeling by ATP-dependent molecular machines. Bioessays **25**:1192-1200.

42. **Mesner, L. D., P. A. Truman, and J. W. Hockensmith**. 1993. DNA-dependent adenosinetriphosphatase A: immunoaffinity purification and characterization of immunological reagents. Biochemistry **32**:7772-7778.

43. **Muthuswami, R.** 1998. DNA-Dependent ATPase A: Overexpression and characterization of the ATP hydrolyzing domain of the enzyme and identification of a novel class of inhibitors specific for this domain.

44. **Muthuswami, R., P. A. Truman, L. D. Mesner, and J. W. Hockensmith**. 2000. A eukaryotic SWI2/SNF2 domain, an exquisite detector of double-stranded to single-stranded DNA transition elements. J.Biol.Chem. **275**:7648-7655.

45. **Narlikar, G. J., H. Y. Fan, and R. E. Kingston**. 2002. Cooperation between complexes that regulate chromatin structure and transcription. Cell **108**:475-487.

46. **Okabe, I., L. C. Bailey, O. Attree, S. Srinivasan, J. M. Perkel, B. C. Laurent, M. Carlson, D. L. Nelson, and R. L. Nussbaum**. 1992. Cloning of human and bovine homologs of SNF2/SWI2: a global activator of transcription in yeast S. cerevisiae. Nucleic Acids Res. **20**:4649-4655.

47. **Quinn, J., A. M. Fyrberg, R. W. Ganster, M. C. Schmidt, and C. L. Peterson**. 1996. DNA-binding properties of the yeast SWI/SNF complex. Nature **379**:844-847.

48. **Reisman, D. N., J. Sciarrotta, W. Wang, W. K. Funkhouser, and B. E. Weissman**. 2003. Loss of BRG1/BRM in human lung cancer cell lines and primary lung cancers: correlation with poor prognosis. Cancer Res. **63**:560-566.

49. **Richmond, T. J. and C. A. Davey**. 2003. The structure of DNA in the nucleosome core. Nature **423**:145-150.

50. **Sambrook, J. and D. W. Russell**. 2001. Molecular cloning: A laboratory manual. Cold Spring Harbor Laboratory Press, New York.

51. **Schalch, T., S. Duda, D. F. Sargent, and T. J. Richmond**. 2005. X-ray structure of a tetranucleosome and its implications for the chromatin fibre. Nature **436**:138-141.

52. **Selby, C. P. and A. Sancar**. 1997. Human transcription-repair coupling factor CSB/ERCC6 is a DNA-stimulated ATPase but is not a helicase and does not disrupt the ternary transcription complex of stalled RNA polymerase II. J.Biol.Chem. **272**:1885-1890.

53. **Shen, X., G. Mizuguchi, A. Hamiche, and C. Wu**. 2000. A chromatin remodelling complex involved in transcription and DNA processing. Nature **406**:541-544.

54. **Stern, M., R. Jensen, and I. Herskowitz**. 1984. Five SWI genes are required for expression of the HO gene in yeast. J.Mol.Biol. **178**:853-868.

55. **Strohner, R., A. Nemeth, P. Jansa, U. Hofmann-Rohrer, R. Santoro, G. Langst, and I. Grummt**. 2001. NoRC--a novel member of mammalian ISWI-containing chromatin remodeling machines. EMBO J. **20**:4892-4900.

56. **Thoma, N. H., B. K. Czyzewski, A. A. Alexeev, A. V. Mazin, S. C. Kowalczykowski, and N. P. Pavletich**. 2005. Structure of the SWI2/SNF2 chromatin-remodeling domain of eukaryotic Rad54. Nat.Struct.Mol.Biol. **12**:350-356.

57. **Tong, J. K., C. A. Hassig, G. R. Schnitzler, R. E. Kingston, and S. L. Schreiber**. 1998. Chromatin deacetylation by an ATP-dependent nucleosome remodelling complex. Nature **395**:917-921.

58. **Tsukiyama, T., J. Palmer, C. C. Landel, J. Shiloach, and C. Wu**. 1999. Characterization of the imitation switch subfamily of ATP-dependent chromatin-remodeling factors in Saccharomyces cerevisiae. Genes Dev. **13**:686-697.

59. **Tyler, J. K. and J. T. Kadonaga**. 1999. The "dark side" of chromatin remodeling: repressive effects on transcription. Cell **99**:443-446.

60. **Vignali, M., A. H. Hassan, K. E. Neely, and J. L. Workman**. 2000. ATP-dependent chromatin-remodeling complexes. Mol.Cell Biol. **20**:1899-1910.

61. **Walker, J. E., M. Saraste, M. J. Runswick, and N. J. Gay**. 1982. Distantly related sequences in the alpha- and beta-subunits of ATP synthase, myosin, kinases and other ATP-requiring enzymes and a common nucleotide binding fold. EMBO J. **1**:945-951.

62. **Wang, W., J. Cote, Y. Xue, S. Zhou, P. A. Khavari, S. R. Biggar, C. Muchardt, G. V. Kalpana, S. P. Goff, M. Yaniv, J. L. Workman, and G. R. Crabtree**. 1996. Purification and biochemical heterogeneity of the mammalian SWI-SNF complex. EMBO J. **15**:5370-5382.

63. **Whitehouse, I., A. Flaus, B. R. Cairns, M. F. White, J. L. Workman, and T. Owen-Hughes**. 1999. Nucleosome mobilization catalysed by the yeast SWI/SNF complex. Nature **400**:784-787.

64. **Wilsker, D., A. Patsialou, S. D. Zumbrun, S. Kim, Y. Chen, P. B. Dallas, and E. Moran**. 2004. The DNA-binding properties of the ARID-containing subunits of yeast and mammalian SWI/SNF complexes. Nucleic Acids Res. **32**:1345-1353.

65. **Wu, L. and F. Winston**. 1997. Evidence that Snf-Swi controls chromatin structure over both the TATA and UAS regions of the SUC2 promoter in Saccharomyces cerevisiae. Nucleic Acids Res. **25**:4230-4234.

Appendix

Luria Broth(LB)(100ml)
Bacterial Peptone 1.0 gm
Yeast Extract 0.5 gm
NaCl 1.0 gm
pH was adjusted to 7.2
For LB agar 1.5 %of Agar was added

Alkaline Lysis solution I
50mM glucose
25mMTris –Cl pH8.0
10mM EDTA,pH8.0
Autoclaved and stored at 4°C

Alkaline Lysis solution II
0.2N NaOH
1%SDS
Solution II is always prepare just before use

Alkaline Lysis solution III
5M Potassium Acetate solution 60mL
Glacial Acetic Acid 11.5mL
Water 28.5mL
The resulting solution is 3M with respect to Potassium and 5M with respect to Acetate

TE, pH 8.0
10mM Tris-Cl, pH8.0
1mM EDTA, pH8.0

TAE(50X,1L)
242 gm Tris Base
57.1 mL Glacial Acetic Acid
100mL of 500mM EDTA pH 8.0

DNA loading Dye(6X)
0.25%Bromophenol Blue
30% Glycerol

SDS-PAGE Running Buffer(1L)
3 gm Tris Base
14.4 gm Glycine
1 gm SD

4X SDS-PAGE Gel Loading Dye
40% glycerol
200 mM Tris-Cl, pH 6.8

800 mM β-mercaptoethanol
8% SDS

30% Acrylamide(100mL)
29gm Acrylamide
1gm Bis-acrylamide
Solution was made in double distilled water and then filter through Whatman filter paper

Phosphate Buffered Saline
137mM NaCl
2.7mM KCl
10mM K_2HPO_4
pH was added to 7.2

Lysis Buffer1
50mM Tris-Cl, pH8.0
200mM NaCl
5% glycerol
1mM β-mercaptoethanol
0.5 mM PMSF
0.1mg/ml lysozyme

Lysis Buffer2
50mM Tris-Cl, pH8.0
50mM NaCl
150mM $MgCl_2$
5% glycerol
1mM β-mercaptoethanol
0.5 mM PMSF
0.1mg/ml lysozyme

Lysis Buffer3
50mM Tris-Cl, pH8.0
50mM NaCl
150mM $MgCl_2$
5% glycerol
1mM β-mercaptoethanol
0.5 mM PMSF
0.1mg/ml lysozyme
0.1%TritonX-114

Lysis Buffer 4
50mM Tris-Cl, pH8.0
50mM NaCl
150mM $MgCl_2$
5% glycerol

mM PMSF
mg/ml lysozyme
ıM β-mercaptoethanol

sis Buffer 5
nM Tris-Cl, pH8.0
)mM NaCl
)mM $MgCl_2$
glycerol
5 mM PMSF
mg/ml lysozyme
ıM β-mercaptoethanol

sis buffer 6
nM Tris-Cl, pH8.0
)mM NaCl
)mM $MgCl_2$
glycerol
5 mM PMSF
mg/ml lysozyme
mM β-mercaptoethanol
%TritonX-114

sis Buffer 7
mM Tris-Cl, pH8.0
) mM NaCl
nM $MgCl_2$
ıM β-mercaptoethanol
mM PMSF
mg/ml lysozyme

G buffer(1X)
mM $TrisSO_4$
ıM$MgSO_4$
ıM β–mercaptoethanol
µg/mL Pyruvate Kinase
ıM PEP

eavage Buffer (1X)
)mM Tris-Cl pH 7.0
50mM NaCl
nM DTT
nM EDTA